4. Biomolecules and Polymers in High Steady Magnetic Fields

Georg Maret and Klaus Dransfeld

With 26 Figures

This is a review of recent progress in our knowledge about the behaviour of synthethic and biological macromolecules and larger biological particles in dilute solution and in the liquid crystalline state, when exposed to strong magnetic fields. Emphasis is on the observation of magnetic orientation as resulting mostly from an anisotropic molecular diamagnetic susceptibility, and on its interpretation in terms of molecular structure, flexibility and intermolecular orientational correlation. Some biological applications of magnetic fields are briefly discussed, including the separation of macromolecules in inhomogeneous fields, the field-induced modification of cellular growth and the field sensitivity of animals.

4.1 Overview

In this chapter we first review briefly the dia- and paramagnetic properties of some organic molecules in Sect. 4.2. Subsequently, Sect. 4.3, we describe recent experiments on the magnetic orientation of various biological materials, polymers, liquid crystals and membranes [4.1]. For example, the magnetic orientation of *long* DNA *chains* (which amounts to about 1% in a field of 20 T) and of other polymers gives direct information about the persistence length or radius of curvature of these macromolecules in solution [4.2]. Shorter segments of DNA or other polyelectrolytic rods (as, for example, virus particles) above a critical concentration form liquid crystalline phases with interparticle distances of up to a few hundred Å. These *polyelectrolytic liquid crystals* can be fully oriented in a strong magnetic field [4.3, 4] and are interesting anisotropic objects for the study both of their dynamics and their structure by scattering of light or neutrons. Furthermore, by evaporating the water from a polyelectrolytic liquid crystal – for example, of virus particles – exposed to a high magnetic field, dry filaments of fully aligned virus molecules have been produced which represent excellent oriented targets for the x-ray structure analysis of the virus itself [4.5].

Biological membranes show strong orientation in a magnetic field due to their intrinsic anisotropic structure. Whether the membrane orients itself parallel or perpendicular to the field depends on the proteins incorporated in the lipid membrane, and the degree of orientation varies whenever phase transitions occur in the membrane. In fact some lipid phase transitions can be observed most

clearly by recording the magnetic orientations as a function of temperature [4.6]. Complex biological structures built up by folded membranes, such as retinal rods [4.7], can be fully oriented in relatively low fields.

High-field magnetic orientation turned out to be useful also for studying molecular structure and phase transitions in classical and polymeric liquid crystals as well as in microemulsions. When a polymer is formed from an oligomer by the addition of monomers *(polymerisation process)* in the presence of a strong magnetic field, the interesting question arises, whether the resulting polymers are oriented. In Sect. 4.4 evidence is presented that both the reaction rate [4.8] and the orientation [4.9] of the final polymer can be enhanced by strong magnetic fields.

We should also mention certain magnetic field dependent *chemical reactions* of great interest [4.10–24]; they are of very different origin and cannot be described here in detail. The reaction rates show a field dependence only at very low fields – between zero field and a few kilogauss at most – but are field independent at higher fields. In most of these reactions, recently reviewed by *Atkins* [4.25, 26] and *Turro* and *Kraeutler* [4.27], the nuclear hyperfine fields of the reacting molecules (10–100 G) are the rate-determining parameters at zero external field but not at much higher fields. Consequently the reaction rate in many cases changes with an applied field only between zero field and a field of several hundred gauss, with no further field dependence at higher fields. Recent developments in magnetochemistry are described in [4.28, 29].

If the magnetic field is strongly *inhomogeneous* diamagnetic macromolecules are expelled from (or attracted into) the regions of the maximum magnetic field, depending on the magnitude of their diamagnetic susceptibility (relative to the solvent). Thus in strong field gradients a separation of macromolecules, proteins or red blood cells from the rest of the solution has been achieved [4.30–32] as described in Sect. 4.5. Perhaps the changes of certain enzymatic activities in an inhomogeneous field observed by *Haberditzl* [4.33] are related to diamagnetic separation of reacting components from each other.

Since high magnetic fields affect the orientation, motion and polymerisation of biomolecules it is not too surprising that a direct *influence of magnetic fields on living cells* also exists. "Magnetobiology" has a long history [4.34–37], but many experimental results in the available fields were contradictory and therefore most of the conclusions appear rather speculative. It is established that certain animals are able to sense the earth's magnetic field and to use it for their orientation (survey in [4.38–42]). In Sect. 4.6 we briefly summarise the significant progress which has been made recently towards better understanding of the detection of such weak magnetic fields by bacteria [4.43, 39], insects [4.38, 44, 45], fish [4.41] and birds [4.40, 42, 46]. Convincing evidence exists that the roots of plants exposed to an *inhomogeneous* magnetic field show an oriented growth towards the low field region [4.47, 48]. We shall also discuss the first observation [4.49] that oriented growth (of monocellular pollen tubes) takes place in *homogeneous* strong fields. We believe that further study of oriented biological growth in high magnetic fields may lead to a better understanding of

the growth process itself, including the mechanism of cell division. Therefore biological experiments in high fields represent in our view a very strong motivation for generating fields in excess of 30 T, particularly since most of the phenomena discussed here vary as H^2.

It goes beyond the scope of this chapter to review in detail the importance of high magnetic fields for high-resolution nuclear magnetic resonance spectroscopy of biological substances. This field of research has rapidly developed since 1960 when the first superconducting 5 T magnets were introduced. Now NMR spectrometers with fields up to 9.4 T have become commercially available and proved to be a powerful tool for structural analysis of many proteins and peptides [4.50–53]. Using high field NMR it has recently been possible to analyse quantitatively the large internal motion within protein molecules [4.54, 55]. In an attempt to improve the resolution and sensitivity of this technique further by working at even higher magnetic fields, a NMR spectrometer using a Nb_3Sn coil for a field of 14 T has recently been tested [4.56]. If one analyses large anisotropic molecules at such high fields they are no longer oriented at random in the solution but show alignment relative to the field. In fact, the complete magnetic orientation of suspended microcrystals of the paramagnetic protein metmyoglobin (Fig. 4.1) made it possible to monitor pseudo single-crystal NMR spectra; thus new structural features could be accurately determined [4.57].

The effects of alternating fields and microwaves on living cells are not discussed here; the reader is referred to the current literature [4.59].

Fig. 4.1. Microcrystals (10–100) μm) of the protein met-aquo-myoglobin suspended in aqueous ammonium sulphate solution are almost completely oriented by a homogeneous magnetic field of only 0.3 T applied for 5 min. The protein carries a high-spin iron in the planar porphyrin group which is responsible for substantial anisotropy of the paramagnetic susceptibility due to some spin-orbit coupling even at room temperature. The observed magnetic orientation is very probably of *para*magnetic origin because microcrystals of *dia*magnetic CO myoglobin do not orient even in 8.5 T [4.57, 58]

4.2 Dia- and Paramagnetic Anisotropy of Macromolecules

If a molecule (without an unpaired electron) is placed in a uniform magnetic field, the intramolecular electronic screening currents generate a diamagnetic moment μ proportional to the magnetic field H

$$|\boldsymbol{\mu}| = \chi |\boldsymbol{H}|,$$

This diamagnetic response is a universal property of matter, only in less than 1 % of the presently known compounds it is overshadowed by a ferromagnetic behaviour [4.60, 61].

The diamagnetic susceptibility of a molecule is closely related to its structure and therefore is generally anisotropic. The diamagnetic moment $\boldsymbol{\mu}$ and the field $\boldsymbol{H}$ are not necessarily antiparallel, but three orthogonal principal axes of the susceptibilty tensor always exist along which $\boldsymbol{\mu}$ and $\boldsymbol{H}$ are antiparallel [4.62]. If χ_{xx}, χ_{yy} and χ_{zz} are the corresponding principal values of the susceptibility in these three directions, the differences $\chi_{zz} - \chi_{xx}$ and $\chi_{zz} - \chi_{yy}$ are the anisotropies $\Delta\chi$ of the molecular diamagnetic susceptibility. The average susceptibility is $(\chi_{xx} + \chi_{yy} + \chi_{zz})/3$ [4.62]. Various definitions and units of diamagnetic susceptibilities are used in the literature. We give some conversions for convenience. The *volumetric* susceptibility χ is defined as the magnetisation M for a sample per unit magnetic field strength H, $\chi = M/H$ in both the cgs Gaussian and the MKSA systems of units. It is dimensionless in both systems and one cgs Gaussian unit of it corresponds to 4π MKSA units. The mass susceptibility χ_g equals χ/m, m being the mass of the sample. The *specific* susceptibility χ_ϱ equals χ/ϱ, ϱ being the mass density, and the *molar* susceptibility χ_m equals $M\chi/\varrho$, M being the molecular weight. Further, χ_m has the dimensions

$$\left[\frac{\mathrm{cm}^3}{\mathrm{mol}}\right] = \left[\frac{\mathrm{erg}}{\mathrm{Oe}^2\mathrm{mol}}\right] = \left[\frac{\mathrm{erg}}{\mathrm{G}^2\mathrm{mol}}\right] \quad \text{or} \quad \left[\frac{\mathrm{m}^3}{\mathrm{mol}}\right] = \left[\frac{\mathrm{J}}{(\mathrm{Am}^{-1})^2}\,\frac{\mathrm{Am}}{\mathrm{Vs}}\,\frac{1}{\mathrm{mol}}\right]$$

$$= \left[\frac{\mathrm{J}}{\mathrm{T}^2}\,\frac{\mathrm{Vs}}{\mathrm{Am}}\,\frac{1}{\mathrm{mol}}\right].$$

The susceptibility per molecule, χ_0, equals χ_m/N_A (with N_A being Avogadro's number) and has dimensions

$$\left[\frac{\mathrm{erg}}{\mathrm{G}^2}\right] \quad \text{or} \quad \left[\frac{\mathrm{J}}{\mathrm{T}^2}\,\frac{\mathrm{Vs}}{\mathrm{Am}}\right].$$

Magnetic orientation involves ratios of magnetic energies to thermal energies per molecule which are

$$\left[\frac{\Delta\chi_0 H^2}{kT}\right] = \left[\frac{\Delta\chi_0 B^2}{kT}\right] \quad \text{or} \quad \left[\frac{\mu_0 \Delta\chi_0 H^2}{kT}\right] = \left[\frac{\Delta\chi_0 B^2}{\mu_0 kT}\right]$$

in the cgs Gaussian or MKSA systems, respectively ($\mu_0 = 4\pi \times 10^{-7}$ Vs/Am). The diamagnetic anisotropy of benzene, for example, amounts to $\Delta\chi = -6.71 \times 10^{-7}$ [cgs Gaussian] or -8.44×10^{-6} [MKSA], $\Delta\chi_\varrho = -7.64 \times 10^{-7}$ [cm^3/G] or -9.60×10^{-9} [m^3/kg], $\Delta\chi_m = -59.7 \times 10^{-6}$ [cm^3/mol] or -7.50×10^{-10} [m^3/mol] and $\Delta\chi_0 = -9.91 \times 10^{-29}$ [erg/G^2] or -1.24×10^{-33} [(J/T^2) (Vs/Am)]. The small differences in $\Delta\chi$ obtained for gaseous, liquid or crystalline benzene with various techniques have been discussed recently [4.63].

The diamagnetic anisotropies of many molecules have been determined directly by producing a single crystal of the molecular species and measuring the torque when the crystal is suspended in a uniform magnetic field [4.64–66]. Other estimates of the diamagnetic anisotropy were derived from measuring the *magnetic birefringence* in the liquid state (Cotton-Mouton effect), provided that the optical polarisability tensor of the molecular was known [4.66–69]. Finally the diamagnetic intramolecular screening currents lead to a reduction of the magnetic field acting on the various nuclei of the molecule. From the corresponding diamagnetic shift of the ^{13}C or ^{1}H lines in *nuclear magnetic resonance* experiments, additional *local* information about the diamagnetic shielding currents within the molecule has been acquired [4.66].

The most striking observation is the large diamagnetic susceptibility χ_{zz} of *aromatic molecules* if the magnetic field is applied perpendicular to the molecular $x-y$ plane. For benzene, for example, the principal molar susceptibilities (in 10^{-6} cm^3/mol) are $\chi_{xx} = \chi_{yy} = -34.9$ and $\chi_{zz} = -94.6$, resulting in an anisotropy of $\Delta\chi = \chi_{zz} - \chi_{xx} = -59.7$. This large value of $\Delta\chi_m$ is caused by the diamagnetic "ring current" which is generated if the field is applied perpendicular to the plane of the conjugated benzene ring [4.70, 77].

For *non-aromatic molecules* (for which a non-local ring current can be excluded) the diamagnetic anisotropy of a molecule is, to a first approximation, the sum of the local anisotropies of the interatomic bonds composing the molecules. For example, one carbon atom has an isotropic susceptibility, but if two carbon atoms are bonded by a single, double or triple bond, this bond has been found to cause diamagnetic anisotropy (Table 4.1), which is of opposite sign for single C–C bonds and for multiple bonds. While a single bond has its largest diamagnetic value for a field parallel to the bond axis and therefore orients perpendicular to the field, the reverse is true for double and triple bonds; they align parallel to the field and show largest diamagnetism for fields

Table 4.1. Observed diamagnetic anisotropies of certain bonds

y ↳ z	$\Delta\chi_m = \chi_{zz} - \chi_{xx}$ [10^{-6} cm^3/mol]	Ref.
C–C	−1.3 (±25 %)	[4.69]
C=C	+8.2	[4.72]
C≡C	+37	[4.73]
C=O	+6.6	[4.74]

perpendicular to the bond axis. As already pointed out by *Lonsdale* [4.64] introduction of double or triple bonds leads to a large *optical anisotropy* with the highest polarisability for the electric field parallel to the bond axis. This latter fact is important for magnetic birefringence experiments.

The diamagnetic anisotropies of other bonds such as the C–H, C–Cl and C–O bonds are less well known. Estimated values obtained mainly from NMR observations are $\Delta\chi_{C-C} \simeq 1 \times 10^{-6}$ [4.75] and $\Delta\chi_{C-H} \simeq \Delta\chi_{C-O} \simeq +3 \times 10^{-6}$ [4.76] [cm/mol]. For further information on many other measurements and theoretical calculations of the diamagnetic anisotropy we refer to the excellent review by *Bothner-By* and *Pople* [4.62]. Of particular interest for the experiments described in Sect. 4.3 are the estimates for the diamagnetic anisotropies of *nucleic acids* and *proteins*. According to calculations by *Veillard* et al. [4.77] the flat *base pairs* adenine-thymine and guanine-cytosine have almost the same diamagnetic anisotropy as a benzene ring with the largest diamagnetism for a field perpendicular to the molecular plane. Recent susceptibility measurements with a sensitive SQUID magnetometer on oriented films of DNA point to somewhat higher values [4.78]. Since in the DNA double helix the base pairs form a parallel stack, a free DNA molecule in a solution orients itself perpendicular to an applied magnetic field, Sect. 4.3.

Recently *Worcester* [4.79] suggested that since the *peptide bond* in proteins partially has the character of a double bond at resonance between the two bond structures, Fig. 4.2, it should have a diamagnetic anisotropy. Based on early experimental data of *Lonsdale* [4.64, 65] he gives $\Delta\chi = +8.8 \times 10^{-6}$ cm^3/mol for the peptide bond. More recently, *Pauling* [4.80] confirmed this anisotropy but arrived at the smaller value $\Delta\chi_m = 5.36 \times 10^{-6}$ cm^3/mol in better agreement with experimental findings [4.81, 82]. Thus the anisotropy of the peptide bond is apparently of the same sign and similar magnitude as for the C=C and C=O double bonds (Table 4.1). Consequently the plane of the peptide bond tends to orient parallel to an external field (as does the plane of the C=C double bond). Since in an α helix the planes of the peptide bonds are parallel to the helical axis, it becomes clear why α helical proteins in solution can align their helical axis parallel to the magnetic field without the assistance of aromatic groups (Sect. 4.2). In addition, three out of the 20 amino acids occurring in proteins (as side groups of the polypeptide chain) are aromatic and therefore have $\Delta\chi$ values comparable to benzene: *Veillard* [4.77] reported the value $\Delta\chi_m = -95.3$ for tryptophane and -60 [10^{-6} cm^3/mol] for both tyrosine and phenylalanine.

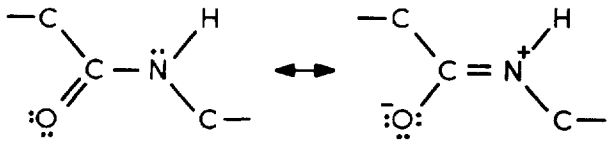

Fig. 4.2. Two bond structures at resonance result in a partial double bond character of the peptide bond

Hence, if coupled in their orientation with respect to the polypeptide chain, aromatic amino acids might contribute substantially to diamagnetic anisotropy in proteins.

If a molecule contains unpaired electrons its overall spin is different from zero, generally resulting in a paramagnetic moment μ. Its paramagnetic susceptibility (per molecule) is then given by *Curie's* law $\chi = \mu^2/3kT$. The term μ is proportional to the g factor which describes the coupling between spin and orbital momentum. For anisotropic groups, such as the iron-containing planar aromatic porphyrin group ("haeme" group), the g factor is usually anisotropic. For example, with strong spin-orbit coupling at low temperatures, g equals 2 normal to the haeme plane whereas $g \sim 6$ within the haeme plane, as deduced from ESR and measurements of the torque in a homogeneous magnetic field on single crystals of myoglobin [4.83]. (For details about the paramagnetic properties of iron-containing proteins we refer to a review article by *Kotani* [4.83].) Interestingly some spin-orbit coupling persists even at room temperature, resulting in a *paramagnetic* anisotropy $\chi_{zz} - \chi_{xx}$ per haeme group which is numerically (for ferri-myoglobin at 300 K) some 30 times higher than the diamagnetic anisotropy of benzene and has *equal* sign [4.83]). *Nakano* et al. [4.84] reported a $\Delta\chi_m$ value of -1100×10^{-6} cm^3/mol for the haeme group in deoxyhaemoglobin. Hence such haeme groups orient substantially better in their paramagnetic than in their diamagnetic state: in both cases they tend to align their planes parallel to the magnetic field. Finally one has to mention the anisotropy caused by the crystal field on the ligands, which could lead to an effective orientation even if the g factor were isotropic.

4.3 Magnetic Orientation of Macromolecular Systems

The orientation of macromolecular systems in magnetic fields is usually caused by their overall anisotropic magnetic susceptibility. Various magnetic orientation effects in liquid crystals have been known for a long time [4.85]. The first experimental evidence for magnetic anisotropy of organised biological structures was found by direct measurements of the torque on mechanically suspended fibres of celluloses, silks, keratines and collagens in a small homogeneous magnetic field in 1942 [4.86]. A similar study on muscle followed in 1958 [4.87]. The magnetic orientability of biological particles in solution was first discovered in 1970 [4.7] by direct microscopic visualisation of the magnetically induced rotation of the outer segments of retinal rods. This work and the report by *Geacintov* et al. [4.88] that the fluorescence of chlorella cells became anisotropic in a strong magnetic field because of magnetic orientation of the chloroplasts [4.89] have triggered a rapid development in this field (Sect. 4.3.4). An interpretation of the early experiments in terms of diamagnetic anisotropy of the constituent subunits was given by *Hong* et al. [4.90a] in 1971. This initiated a discussion about the relative contributions of diamagnetic anisotropies of lipids, aromatic amino acids, α-helical parts of proteins and

chromophores in these complex biological objects. Clarification resulted mainly from orientation studies on simpler systems such as α-helical polypeptides: they form liquid crystalline phases and therefore are substantially orientable already by *small* magnetic fields [4.91] (Sect. 4.3.2). Alcanes and phospholipids generally require stronger magnetic fields and more sophisticated optical techniques for orientation to be detected [4.6] (Sect. 4.3.4). It is now possible to investigate by *high* field magnetic birefringence the structure of smaller isolated particles like viruses in dilute solution [4.92] (Sect. 4.3.5). High magnetic fields have also become important in the study of intra- and intermolecular orientational correlations in liquids. For example, the rigidity of polymer chains has been studied in various dilute polymer solutions (Sect. 4.3.2a): long-range order due to intermolecular interactions was investigated in solutions of charged polymers ('polyelectrolytes'), in polymer melts (Sect. 4.3.2b) and in thermotropic liquid crystals near the isotropic-nematic transition temperature (Sect. 4.3.3). Some of this work was briefly reviewed recently [4.93].

4.3.1 Magnetic Birefringence, Cotton-Mouton Effect

The magnetic anisotropy of small molecules is weak and even in strong magnetic fields only modest alignment occurs. The deviation from random orientations of the molecules results in an optical birefringence (Cotton-Mouton effect) which can be measured with extreme sensitivity (Fig. 4.3). This is perhaps the most sensitive way to detect magnetic orientation in liquids and gases.

The theory of the Cotton-Moutton effect of *independent rigid molecules* was first developed by *Langevin* [4.95] and *Born* [4.96] and was extended later on [4.67, 68, 97, 98]. We summarise first the simple case of non-interacting rotationally symmetric molecules with anisotropic diamagnetic susceptibility ($\Delta\chi_0$) and optical polarisability ($\Delta\alpha_0$). Let $f(\theta)$ be the magnetic field dependent orientation distribution function of the molecules which is given by Boltzmann statistics, and θ is the angle between the magnetic field direction and the molecular z axis. Each molecule of the ensemble at angle θ contributes on the average $(3\cos^2\theta - 1)\Delta\alpha_0/2$ to the macroscopic optical anisotropy. Integration of the latter function weighted with $f(\theta)$ results in the effective optical anisotropy per molecule; for $\Delta\chi_0 H^2 \ll kT$ it turns out to be

$$\Delta\alpha_0 \cdot \frac{\Delta\chi_0 H^2}{15kT} = \Delta\alpha_0 \cdot \Phi.$$

The term Φ is sometimes called degree of orientation. With the Lorentz-Lorenz formula (relating polarisability and refractive index) the magnetic birefringence Δn becomes in cgs Gaussian units[1]

---

1 in MKSA units (4.1) becomes

$$\Delta n = \frac{1}{18\varepsilon_0} \frac{(n_0^2+2)^2}{n_0} N\Delta\alpha_0 \frac{\mu_0 \Delta\chi_0 H^2}{15kT}.$$

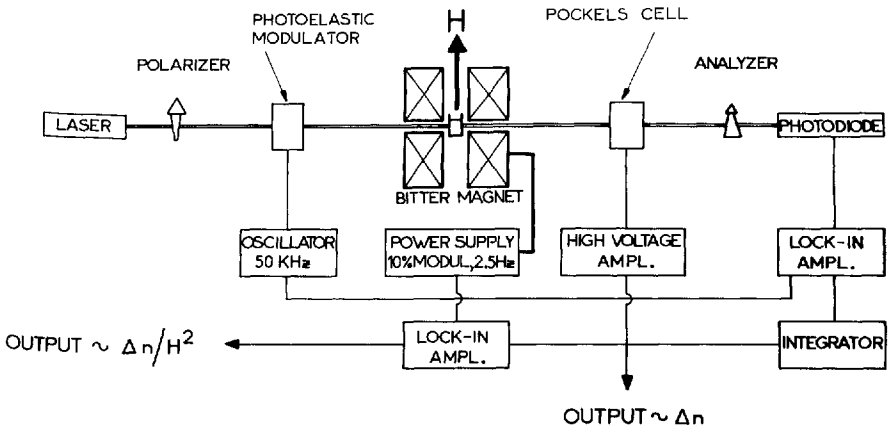

Fig. 4.3. Sensitive magnetic birefringence setup. Laser light (usually 632.8 nm wavelength) propagates horizontally through the sample in a vertical magnetic field (≤ 13.5 T) produced by a Bitter solenoid with 4 mm horizontal and 5 cm vertical bore. Polarizer and analyzer are crossed and at 45° with respect to H. A small 50 kHz modulation of the birefringence is produced by a photoelastic modulator resulting in a 100 kHz intensity modulation of the photodiode output. Any superimposed steady state (magnetic) birefringence results in an additional 50 kHz photodiode output which is phase-sensitively detected, dc converted and used as error signal in a feedback loop to compensate the steady state birefringence, by a Pockels cell. Hence in the compensated mode the voltage across the Pockels cell is a direct measure of the magnetic birefringence Δn. A low-frequency modulation of H induces a LF modulation of Δn which is directly proportional to the Cotton-Mouton constant and can be detected continuously by a second lock-in amplifier. At a sample length of 1 cm (sample volume ~1 ml) the resolution in Δn is close to 10^{-10} for transparent liquids. It is essentially limited by mechanical vibrations of the hydraulic cooling system of the *Bitter* coil [4.94]

$$\Delta n = \frac{2\pi}{9} \cdot \frac{(n_0^2+2)^2}{n_0} N \Delta\alpha_0 \frac{\Delta\chi_0 H^2}{15kT} = \Delta n_{\text{sat}} \Phi. \tag{4.1}$$

Here n_0 is the mean refractive index of the solution, $N = cA_0/M$ is the number of molecules per unit volume, c, A_0, M are concentration, Avogadro's number and molecular weight, respectively and Δn_{sat} denotes the birefringence of a completely oriented sample. The general validity of the Lorentz-Lorenz description of the local optical electric field is not clear. Field corrections are frequently ignored for macromolecular solutions and hence

$$\Delta n = \frac{2\pi}{n_0} N \Delta\alpha_0 \frac{\Delta\chi_0 H^2}{15kT} \tag{4.2}$$

is used instead of (4.1). The Cotton-Mouton constant CM is defined for sufficiently small magnetic fields by

$$\Delta n = \text{CM} \lambda H^2, \tag{4.3}$$

with λ being the wavelength of light. The variation of Δn or Φ in stronger fields and its saturation can be found in [4.97, 99, 100]. Briefly, Φ tends towards $+1$ (or -0.5) for molecules aligning parallel (or perpendicular) to the field.

The Cotton-Mouton effect of dense liquids of low molecular weight and of some gases has been extensively studied during the past 60 years [4.62, 63, 67, 98, 101].

We consider now correlations of the orientation of the N molecules. The most simple case is non-interacting *rodlike stacks* consisting of say N_0 molecules with z axes parallel to the rod axis in each stack. With the current assumption of additivity of the diamagnetic and optical anisotropies, these stacks have anisotropies $N_0\Delta\chi_0$ and $N_0\Delta\alpha_0$. Because their number density is N/N_0, the rhs of (4.1) has to be multiplied by N_0 and hence their magnetic birefringence and orientation is N_0 times higher at identical N. A non-parallel orientation of the molecules within the stack reduces the Cotton-Mouton constant. For example, a rotationally symmetric arrangement of molecules having an angle δ between their z axes and the symmetry axis of the stack reduces CM by

$$(\tfrac{3}{2}\cos^2\delta - \tfrac{1}{2})^2.$$

If the freely rotatable object is an anisotropic *cluster* (or domain) of a certain spatial extension – the so-called orientational correlation length – involving an effective number N_1 of parallel molecules, the rhs (4.1) has to be multiplied by N_1.

In the more complicated case of (isolated) *flexible polymer* chains products of the monomeric diamagnetic susceptibility tensor and the optical polarisability tensor have to be averaged over all possible conformations of the chain [4.102, 103]. A simpler approach was chosen by *Stuart* and *Peterlin* [4.104] in 1950. The actual chain was replaced by an equivalent chain built up of rigid segments, the "*Kuhn* statistical segments", each of which can be freely rotated relative to the neighbouring segments. The segmental length l_s is usually larger than the actual monomer length l_0 (but shorter than the length L of the fully extended chain). The l_s increases with the chain rigidity in such a way that for long chains ($L \gg l_s$) the mean overall extension (radius of gyration) of the real chain and the model chain are identical [4.103]. Stuart and Peterlin considered the *Kuhn*-segment as rods orienting independently in a magnetic field and hence their result corresponds to (4.1), if $\Delta\chi_0$, $\Delta\alpha_0$ and N are replaced by $\Delta\chi_0 \cdot l_s/l_0$, $\Delta\alpha_0 l_s/l_0$ and $N \cdot l_s/l_0$, respectively. The Cotton-Mouton constant of the polymer is l_s/l_0 times higher than the value for independent monomers. This rather qualitative model has been frequently applied to CM measurements of dilute polymer solutions [sometimes corrected for a non-rotationally symmetric orientation of (side) groups with respect to the segmental direction]. The resulting l_s values can be considered as an order-of-magnitude estimate for the orientational correlation length along the polymer chain.

Another description of a long chain molecule dates back to *Kratky* and *Porod* [4.103], appropriate for *semiflexible* chains. The chain bends in a characteristic

homogeneous "worm-like" fashion and the parameter describing its rigidity is the persistence length P. It is defined as the chain's end-to-end vector averaged over all chain configurations and in the limit of vanishing segmental length [4.103], and is proportional to the bending elastic modulus of the chain [4.105]. The *Kuhn* and *Kratky-Porod* models are related by $2P \triangleq l_s$ [4.103]. *Wilson* [4.106] and *Weill* [4.93] have calculated the Cotton-Mouton constant for the "worm-like" model by the appropriate tensor averaging [4.102]. It turns out [4.93] that the rhs of (4.1) has to be multiplied by

$$\frac{l_0}{L} \sum_i \sum_j \left\langle \frac{(3\cos^2 \theta_{ij} - 1)}{2} \right\rangle ,$$

θ_{ij} being the angle between the directions of the ith and jth chain segment, and $\langle\ \rangle$ denoting averaging over all configurations. *Wilson* and *Weill* end up with the identical result in the case of long chains ($P \ll L$): the polymeric Cotton-Mouton constant exceeds the monomeric value by $2P/3l_0$, and is independent of the polymeric molecular weight. Such a tensor averaging for *Kuhn*'s segmental chain and ($l_s \ll L$) results in $l_s/3l_0$ instead of l_s/l_0. In the limit of short chains ($P \gg L$), rod-like behaviour is found and CM is proportional to the molecular weight (L/l_0). *Weill* has given an analytic expression of the above double sum for any chain length:

$$\frac{l_0}{L} \sum \sum \langle\ \rangle = \frac{2P}{3l_0} \left\{ 1 - \frac{P}{3L} \left[1 - \exp\left(-\frac{3L}{P} \right) \right] \right\}. \tag{4.4}$$

Therefore, the persistence length of polymers can now be determined without knowledge of $\Delta\alpha_0$ and $\Delta\chi_0$ from CM measurements on two (or more) fractions of suitable and well-known L. One can sometimes use solutions of monomers and high molecular weight polymers for this purpose.

For very flexible polymers the worm-like model is less appropriate. Bond angle restrictions require more *specific models* such as the, so-called, rotational isomeric state model [4.103]. Cotton-Mouton constants can be calculated in analogy to the electro-optical Kerr constant (electric birefringence).

4.3.2 Polymers

a) Isolated Chains

Some experimental Cotton-Mouton constants of dilute polymer solutions are summarised in Table 4.2. A chemically simple polymer is *polyethylene* $(CH_2)_x$ (Fig. 4.4). The diamagnetic bond anisotropy of C–C is very small (Sect. 4.2), but still much larger than the C–H anisotropy [4.66, 69]. This combined with the high chain flexibility results in a very weak Cotton-Mouton constant in dilute solution [4.107, 108], which is in good agreement [4.98, 107, 108] with the rotational isomeric state model [4.106]. At concentrations $\geq 40\,\%$ in CCl_4 an

Table 4.2. Cotton-Mouton constants and persistence length of some polymers in dilute solutions[a]

Polymer	See Fig.	Solvent	Specific CM const. ($10^{-13}\,G^{-2}\,cm^{-1}$ per mass fraction)	Ref.	Chain model	Persistence length [nm]
$(CH_2)_{16}H_2$	4.4a	Carbon tetrachloride	0.25	[4.69, 107, 108]	Rational isomeric state [4.103]	–
Polycarbonate	4.5	Chloroform	9.6	[4.107–109]	Worm-like [4.93, 106] Kuhn [4.104]	2.7 $(l_s/2)=1.7$
Polystyrene	4.4b	Benzene	6.8	[4.110]	Rational isomeric	–
		teteachloroethylene	12.7	[4.110]	state [4.111]	–
Poly-p-benzamide	4.7a	Conc. H_2SO_4	125	[4.107, 108]	Worm-like [4.93, 106]	75
Poly-1.4-phenylene-terephtalamide	4.7b	Conc. H_2SO_4	200	[4.107, 108]	Worm-like [4.93, 106]	120
Various mesogenic polyesters	4.8	1,1,2,2-Tetra-chloroethane	9–18	[4.112]	–	–
Poly(Tyr-Glu)	4.9	H_2O, $\mu=1.1\times10^{-2}$ M	93	[4.113]	Worm-like [4.93, 106]	20
		H_2O, $\mu=$ 10^{-1} M	22			4
Polystyrene sulphonate	–	H_2O, $\mu=2$ M	2.6	[4.114]	Worm-like [4.93, 106]	1.2
DNA	4.10	H_2O, $\mu=10^{-3}$	460	[4.2, 6, 115]	Worm-like [4.93, 106]	113
		H_2O, $\mu=10^{-2}$ M	290			71
		H_2O, $\mu=$ 1 M	280			69

[a] μ=ionic strength; all CM values measured at room temperature and $\lambda=632.8$ nm

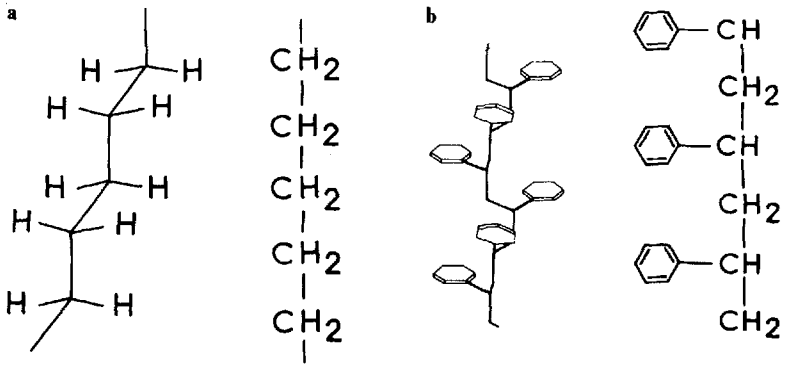

Fig. 4.4. (a) Polyethylene, (b) Polystyrene

onset of interchain correlations was observed (Sect. 4.3b), possibly related to a particular intermolecular correlation of the CCl_4 molecules [4.116].

Polycarbonates (Fig. 4.5) show a specific Cotton-Mouton constant almost 40 times higher than the alcanes [4.107–109], mainly due to the large $\Delta\chi$ and $\Delta\alpha$ values of the *in-chain* phenyl group. *Stamm* [4.107] and *Champion* et al. [4.109] derive different chain rigidities from identical experimental results (Table 4.2). Part of the problem is related to the reliable determination of effective diamagnetic and optic anisotropies with respect to the axis of the polymeric backbone. *Champion's* approach [4.109] is to combine magnetic and flow birefringence data with estimated $\Delta\alpha_0$ and $\Delta\chi_0$ values of the phenyl group; the resulting information about the local conformation of the backbone and the segmental length stems from the application of the *Stuart-Peterlin* theory. *Stamm*'s CM data of polymeric polycarbonate and of a monomeric model compound result in $P=2.7$ nm, when analysed according to the worm-like model see Eqs. (4.1, 4). This P value seems to be a lower limit because the above treatment certainly somewhat overestimates the effective $\Delta\alpha \cdot \Delta\chi$ value.

If the predominant anisotropic group, such as the phenyl group of *polystyrene* (Fig. 4.4b), is located in a side chain of the polymer, the analysis of Cotton-Mouton data in terms of polymeric backbone rigidity is less obvious. The degree of rotational mobility of the side group with respect to the main chain should be known from other sources. It should not be too high since otherwise the effective anisotropy along the backbone becomes small. The rotational freedom of the phenyl side group of polystyrene is known to be restricted [4.111, 117, 118]. The CM values of polystyrene in benzene (or tetrachlorethylene) (Table 4.2 and Fig. 4.6) exceed the monomeric Cotton-Mouton constant (i.e. essentially benzene) by a factor of 1.4 (or 2.6, respectively). This compares with a correlation parameter of 1.69 calculated by *Tonelli* et al. [4.111] based on the rotational isomeric state model and confirms the great flexibility of polystyrene in solution. In contrast, large CM values combined with strongly non-linear magnetic birefringence curves were reported for polystyrene in

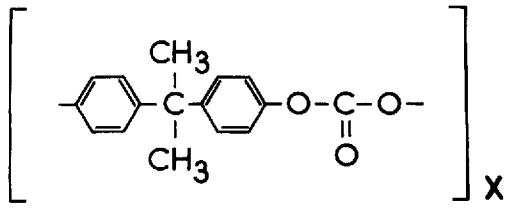

Fig. 4.5. Polycarbonate (Biphenyl -A-Pc)

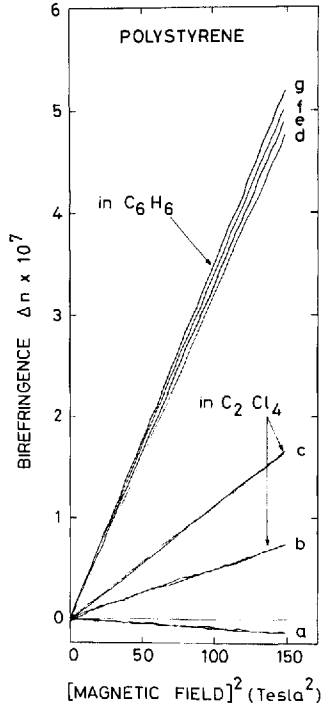

Fig. 4.6. Cotton-Mouton effect of solutions of polystyrene in *tetrachloroethylene* (*a*) $c=0$, (*b*) $c=7\,\%$, (*c*) $c=15\,\%$ and in *benzene* (*d*) $c=0$, (*e*) $c=7\,\%$, (*f*) $c=14\,\%$, (*g*) $c=21\,\%$, $T=22^{\circ}$, $\lambda=632.8$ nm, optical path $=3$ cm, [4.110] ▶

cyclohexane and benzene, suggesting the existence of micron-sized aggregates in these samples [4.119]. As such anomalies have never been found by others [4.107, 108, 110, 120] we feel they are related to impurities.

Polybenzamides have been investigated by *Tsvetkov* et al. [4.121] and *Stamm* [4.107] in sulphuric acid, in 1-methylpyrolidon (MP) and in dimethyl-acetamide (DMAA) with LiCl. These polymers are of special interest because they have high mechanical and thermal strength and are liquid crystalline in concentrated solutions, resulting in various technological applications (for example, high modulus "Kevlar and Nomex fibres"). From low-field CM measurements, using the Stuart-Peterlin approach, Tsvetkov et al. suggested a persistence length of more than 500 nm ($l_s \geq 1000$ nm) for PBA (Fig. 4.7) in concentrated H_2SO_4. From precise high field CM measurements Stamm found (at concentrations below 2 %) P values of 75.0 nm (120 nm) for PBA (PPTA, Fig. 4.8) applying the worm-like chain model. He also found [4.107] conformational changes of PBA in DMAA (at ionic strengths above 1.5 % LiCl) and states with intermolecular order.

Interesting applications are expected from polymers carrying so-called mesogenic groups in the main chain which favour liquid crystalline order (Fig. 4.8). These new polymers have liquid crystalline phases in the melt at temperatures well below the onset of chemical decomposition (Sect. 4.3.2b).

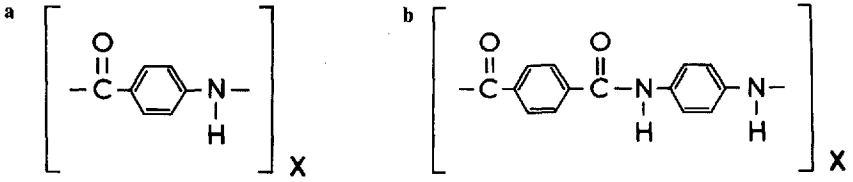

Fig. 4.7. (a) Poly-p-benzamide; (b) Poly-1,4-phenylene-terephtalamide

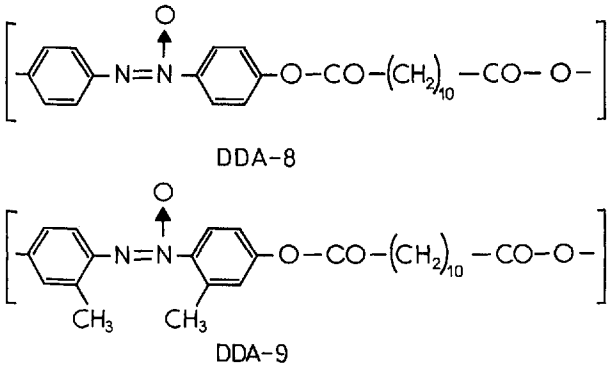

Fig. 4.8. Two polyesters with "mesogenic" groups and flexible spacers in the main chain. Both DDA-8 and DDA-9 [4.112] have liquid crystalline (or "meso"–) phases in the melt

Cotton-Mouton experiments have shown so far [4.112] that individual chains of these polymers in dilute solution have no tendency to form intrachain order (such as backfolding of mesogenic segments). They are highly flexible random coils in solution.

We now turn to polymers in aqueous solutions. In water, chemical dissociation of some polar groups usually occurs and an electrically charged macromolecule is obtained surrounded by small "counter" ions of opposite polarity. Such solutions which sometimes contain additional salt (i.e. additional ions of both polarities) are called *polyelectrolytic*. Almost all biopolymers are polyelectrolytes. At high charge density of the macroion and low counterion concentrations (i.e. weak screening) the chain conformation and the persistence length are determined by long-range electrostatic interactions between segments of the chain. At low charge densities and high counterion concentrations (i.e. strong screening) the chain can be considered neutral and its conformation is given by its local "steric" rigidity. This electrostatic effect has been known qualitatively for a long time. A theoretical description of the electrostatic persistence length of polyelectrolytes has been advanced recently [4.122–124 and references therein]. Various experimental techniques such as flow birefringence, dichroism [4.125, 126] and electro-optic relaxation [4.127, 128] have since been employed to check the predictions, showing the actuality of this basic problem.

We believe that *magnetic* birefringence is particularly well suited for studying polyelectrolytes since it has many intrinsic advantages when compared to electric field induced orientation techniques. For example, (a) the local magnetic field is very well known. It equals the external field within about 10^{-6} in the usual case of diamagnetic solutes and solvents. (b) It can be applied "steady state" and orientation can be studied in true thermal equilibrium. (c) There is only one well-defined orientation mechanism, described by (4.1), and (d) diamagnetic anisotropies are additive quantities to a good approximation (Sect. 4.2). (e) Very small amounts of sample are needed. In general, (a–e) are not true when electric or flow fields are applied to electrolytic solutions. However, the degree of molecular alignment obtained in strong magnetic fields is sometimes comparatively poor; even with sensitive birefringence techniques single-chain properties at sufficiently low concentrations sometimes can hardly be investigated. Obviously stronger steady magnetic fields could be helpful.

Cotton-Mouton experiments are available on the rather flexible polypeptide *polytyrosine glutamic acid* (Fig. 4.9) [4.113], on *polystyrene sulphonate* [4.114] and on *nucleic acids* (Fig. 4.10) [4.2, 6, 94, 129]. Poly (Tyr-Glu) carries the aromatic tyrosine in the side group; since the side group mobility is unknown the absolute persistence length cannot be deduced from CM measurements. A strong electrolytic stiffening is probably responsible for the increase of CM at low ionic strengths (Table 4.2).

The Cotton-Mouton constant of polystyrene sulphonate at high ionic strength is very weak and does not depend on ionic strength. This corresponds to a "steric" persistence length of about 1.2 nm [4.114]; its increase observed at

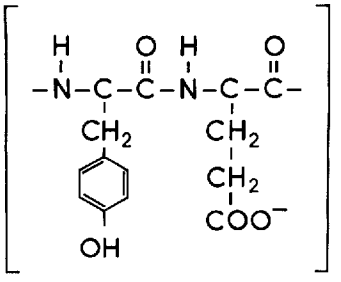

Fig. 4.9. Poly-tyrosine-glutamic acid

Fig. 4.10. Double-helical DNA [4.130]

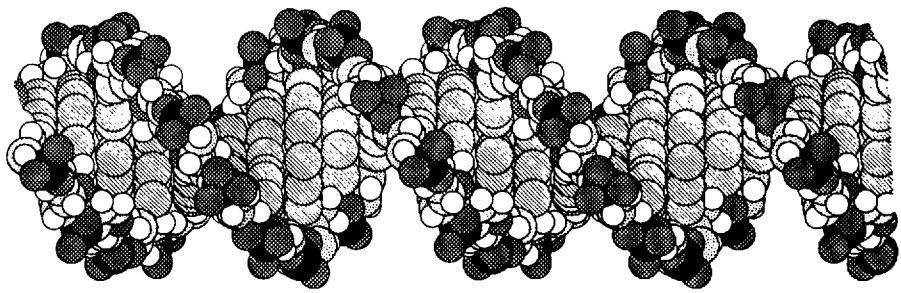

lower *ionic* strength is due to the electrostatic stiffening of individual chains and quantitatively agrees with the theoretical predictions [4.122, 124]; it becomes molecular-weight dependent because at low ionic strength Debye's electrostatic screening length is no longer small compared to the chain length L [4.114].

For DNA an increase of CM at ionic strength below some 10^{-2} M NaCl was reported earlier [4.6]. New measurements performed with improved experimental resolution and at lower concentrations enabled lower ionic strengths to be explored; it turned out [4.94] that the electrostatic persistence length deduced agrees with the *Odijk* theory over an ionic strength range of more than 3 orders of magnitude. At high ionic strength the Cotton-Mouton constant runs into a plateau given by the "steric" persistence length. The P values (Table 4.2), obtained by using the now well-established values $\Delta\alpha_0 = 12.8 \times 10^{-24}\,\mathrm{cm}^3$ per base pair [4.131] and the preliminary experimental $\Delta\chi_0 \approx 90\,\mathrm{cm}^3/\mathrm{mol}$ [4.78], agrees fairly well with results from other techniques [Ref. 4.132 and references therein]. Changes in rigidity with external parameters, for example during thermal denaturation, can be monitored directly by the Cotton-Mouton constant [4.2].

b) Interacting Chains

This section deals with ordering phenomena occurring at higher polymer concentrations. Knowledge about long-range intermolecular order and the forces involved are important for understanding not only macroscopic properties of liquid crystals, gels and polymer melts, but also biological processes like protein self-assembly and cell division. Intermolecular forces inducing parallel arrangements of molecules result in an increase of the magnetic orientability. Therefore strong magnetic fields have a broad variety of applications: they range from sensitive detection of the onset of weak orientational correlations to full macroscopic orientation of a sample with well-developed long-range order.

It is well known that charged *spherical* particles with typical diameters of 100 nm organise themselves in water above a critical concentration. They may form Wigner-type lattices with concentration-dependent lattice constants of many diameters because of their mutual electrostatic repulsion [4.133, 134]. Rod-like particles such as tobacco mosaic virus (length ~ 300 nm, diameter ~ 20 nm) at elevated concentrations show an almost parallel, liquid crystal-like, orientation extending over large domains [4.135–139]. *Onsager* in 1949 [4.140] was the first to predict such ordered phases of rods on the basis of entropy arguments. Considering only hard core interactions, he calculated two critical concentrations for the onset and full development, respectively, of the anisotropy. Both are inversely proportional to the rod length. Much theoretical work including work on semiflexible chains is available now [4.141, 142]. However, in the charged-rod water systems ordering has been observed already at substantially lower concentrations than predicted by hard core theories; hence more long-range (electrostatic and eventually electrodynamic) forces are probably involved [4.143–147]. In spite of the experimental and theoretical progress in this field a satisfactory quantitative description of both the electrostatic and the van

der Waals potential between the macromolecules is still missing. For example, it is not yet clear how the long-range superstructure sometimes observed in such solutions can be related to the macromolecular structure; is there a general relation between the superstructure and the helical structure of the macromolecule at substantial dilution? Is the spatial extension of order connected to the macromolecular flexibility? In the following section we shall illustrate the potential value of high magnetic fields in this research area by summarising some experiments on concentrated polyelectrolytes.

I) Polyelectrolytic Solutions

Poly(Tyr-Glu) is a rather flexible polyelectrolyte at solvent conditions as mentioned above (Sect. 4.3.2a). Despite this, a transition into a phase of locally parallel ordered chains (involving interchain interactions) is suggested from the observation of a *sudden increase of the magnetic birefringence* at concentrations around 2.5 % [4.113]. Neutron scattering data were consistent with a mean radial intermolecular distance of about 6 nm in this case and the order seemed to extend only over a few hundred Kuhn segments. The observed sharp decrease of CM with ionic strength indicates the importance of electrostatic interaction for parallel ordering. Many currently studied polyelectrolytes, such as polystyrenesulphonate, have flexibilities, charge densities and diamagnetic anisotropies comparable to Poly(Tyr-Glu). Unfortunately most of them cannot be oriented in magnetic fields easily and have an undefined flexibility which depends on the solvent parameters.

Therefore very long thin charged rod-like *bacteriophages* (Pf1, fd) were studied *as model systems* [4.3, 92, 148]. They have a highly ordered internal structure resulting in a large diamagnetic anisotropy (Sect. 4.3.5) and form large birefringent domains at concentrations above about 1 % (Fig. 4.11a); at the critical concentration the Cotton-Mouton constant suddenly increases by more than 3 orders of magnitude [4.3] and saturation of the magnetic birefringence is observed in fields of about 5 T (Fig. 4.12). The rods are aligned essentially parallel to the magnetic field and may maintain their macroscopic orientation for hours at zero field (Fig. 4.11b), so enabling investigation of the structure and dynamics of the oriented polyelectrolytic liquid crystal by small-angle neutron and light scattering [4.3, 148–150]. The result indicates parallelism of the rods; in the radial direction a liquid-like structure factor is found with a well-defined concentration-dependent ($c^{-1/2}$) average next-neighbour distance of up to 70 nm. The effective diameter of rods deduced from the experimentally excluded volume is about 3 times larger than their geometric diameter, reflecting the thickness of the ionic cloud; it is however still about two times smaller than the mean radial next-neighbour distance, suggesting substantial freedom of non-collective lateral and axial motions. In the axial direction distances are random, no smectic-like layer structure could be found [4.149, 150], the light scattering is dominated by single-particle interference. Quasielastic light-scattering experiments by *Oldenbourg* reveal [4.149, 150] a strongly anisotropic translation

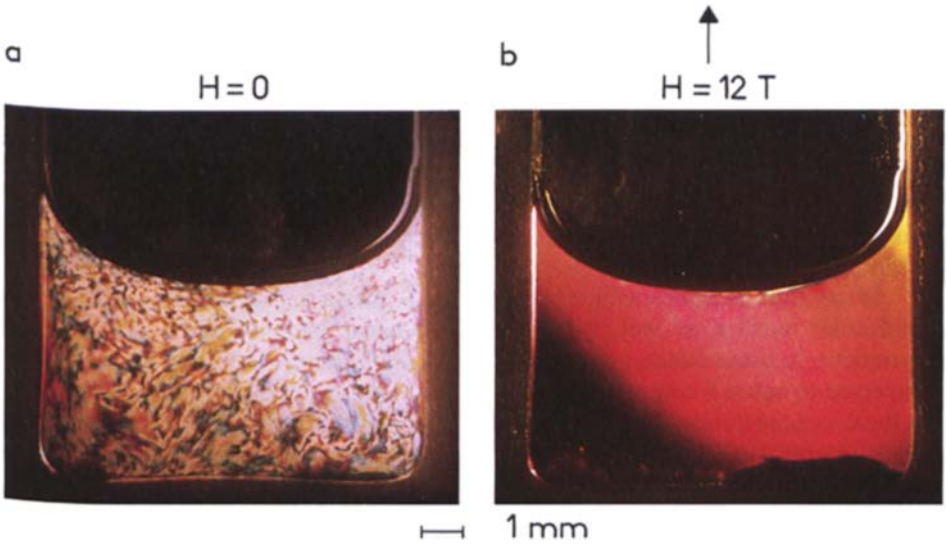

Fig. 4.11a, b. In solutions of the highly charged rod-like virus particle Pf1 (length ~1980 nm, diameter ~6 nm, pH 7.5, 10 mM Tris HCl, $T = 20\,°C$), a long-range parallel ordering of rods occurs above a critical concentration of ~0.6 % w/w. The preferential radial next-neighbour distances (~33 nm at $c = 2.4\,\%$ w/w) are maximised, corresponding to homogeneous space filling large birefringent domains which are (**b**) completely oriented in a magnetic field above ~5 T [4.148]. Photographs of 1 cm wide cells with 0.1 cm optical path between diagonal crossed polarisers were taken before (**a**) and after (**b**) exposure to a vertical magnetic field of 12 T ($c = 2.4\,\%$ w/w). The magnetic orientation is maintained in zero field for minutes to hours depending on the environment (temperature gradients, shaking). Similar ordering effects occur in solutions of a shorter bacteriophage fd (length 880 nm, diameter 6 nm) at concentrations above ~1.1 % w/w [4.3, 92, 148–150]

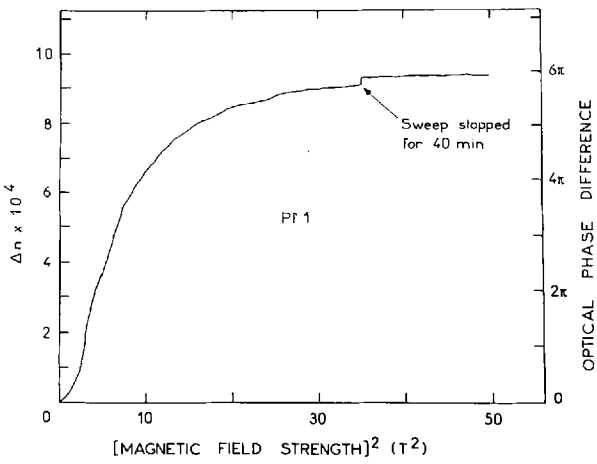

Fig. 4.12. Magnetic birefringence of the rod-like bacteriophage Pf1 in a liquid crystalline aqueous solution (at $c = 14.8$ mg/ml, $T = 20\,°C$, $\mu = 10$ mM Tris HCl, $\lambda = 632.8$ nm, optical path = 0.2 cm, field sweep velocity = 6.2×10^{-4} T/s). The arrow indicates a 40 min stop of the magnetic field sweep. After this time no further increase in Δn is observed

diffusion coefficient. Axial diffusion (along the magnetic field) is close to the free diffusion which would occur along the rod axis in isotropic solution, whereas the complex radial diffusion behaviour – involving two very different relaxation modes – indicates strong interparticle interaction. Our present view of the ordered phase of bacteriophages is that of a very "soft" lyotropic nematic, the large excluded volume of the rods being controlled by the counterion cloud. Observing full and stationary magnetic orientations of this system facilitates not only the production of oriented fibres (Sect. 4.4) but makes possible studies of anisotropic electrolytic properties like ionic fluctuations and ionic densities in ordered polyelectrolytes.

Many rigid or semiflexible polyelectrolytes have a helical conformation; the molecular surface as well as the surface charge should reflect the helical symmetry to some extent, and any intermolecular interaction of this symmetry is expected to cause a complicated *twisted long-range order* in solutions above the critical concentration. Long-range order with periodicities much larger than both intermolecular distances and molecular lengths has been observed and studied in some detail in polyelectrolytic solutions of the bacteriophage fd [4.149, 151], nucleic acids [4.3, 4, 151–155] and in the helical polysaccharide xanthan [4.156].

For fd and xanthan the *long periods* range from 10 μm to several 100 μm depending on concentration and ionic strength. They are easily measurable with laser light diffraction or can be seen in a polarising microscope; two examples are shown in Fig. 4.13. Combined measurements of optical rotation, birefringence and scattering of light and neutrons clearly demonstrate that the xanthan and fd rods are organised like the molecules in a neat cholesteric liquid crystal (Fig. 4.14) except for a much larger lateral interparticle distance.

Just as in classical cholesteric liquid crystals, molecules are parallel within planes, but have mean radial distances and interplane spacings d up to 10 times larger than the rod diameter. The twist angle between molecules in neighbouring planes defines a screw with periodicity along the direction A – A, the cholesteric axis. Since individual rods have different axial and radial refractive indices, the birefringence is modulated with period D along the cholesteric axis; the bright-dark layers seen in Fig. 4.13 are due to this birefringence modulation and thus make *visible* the planes normal to the cholesteric axis.

Various *magnetic field effects* occur in cholesteric liquid crystals. They have been extensively discussed in the literature [4.1, 85, 152, 157], so we mention only those relevant to the present experiments on polyelectrolytes. When orientational constraints due to wall effects can be neglected, the cholesteric axis for molecules with $\Delta\chi < 0$ or $\Delta\chi > 0$ tends to align parallel (a) or perpendicular (b) to H. In case (a) once all molecules are aligned normal to H by this process no further effects take place in stronger fields. The period D is magnetic field independent. In (b) even for complete alignment of all A – A axes normal to H many molecules are still not oriented along H. Hence in stronger fields when the magnetic torque on the non-aligned molecules becomes comparable to the restoring elastic torque for planar twist (Sect. 4.3.3c) the cholesteric screw

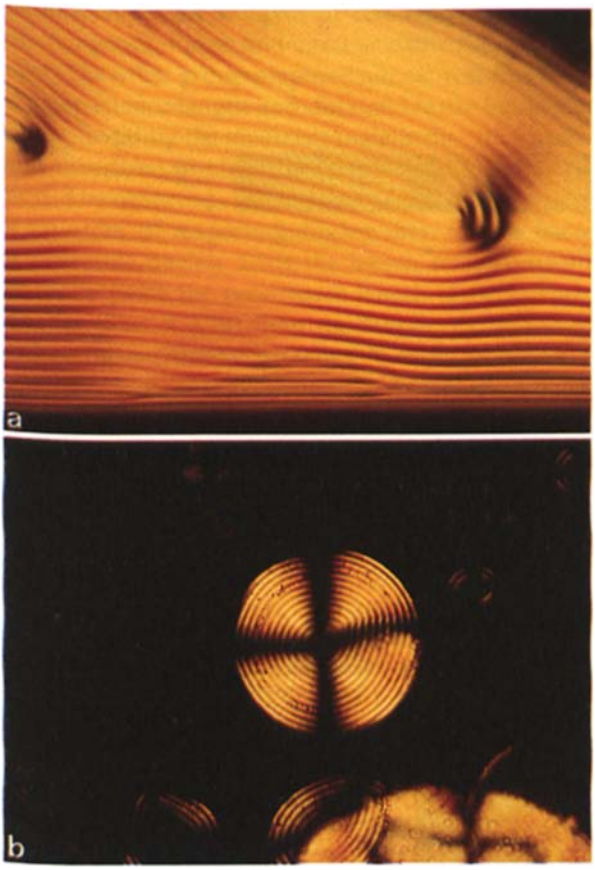

Fig. 4.13a, b. Microphotographs of ordered polyelectrolyte solutions in 0.1 cm thick optical cells between horizontal and vertical polarisers using white light. (**a**) Solution of the rod-like bacteriophage fd at 20 mg/ml in 10 mM Tris HCl, pH 7.5. The rods are ordered as in a cholesteric liquid crystal (Fig. 4.14) with lateral next-neighbour distances of ~33 nm (~5.5 diameters) on the average here. The cholesteric period (2D) is 61 μm [4.149]. (**b**) Helical semi-rigid xanthan molecules also form a cholesteric polyelectrolytic phase; at a concentration of 116 mg/ml the period (2D) is about 12 μm. Between the first and second critical concentration for the onset and full development of the cholesteric phase, respectively, a phase separation is observed and anisotropic droplets, surrounded by less concentrated isotropic solution, can be seen. They have a spherical shape apparently due to surface tension, resulting in a very distorted twisted structure similar to the "spherolites" in solutions of PBLG [4.139]. Note that a spherical structure with radial cholesteric axes everywhere is topologically impossible, in accordance with the observation of one radial line of defects in each droplet [4.156]

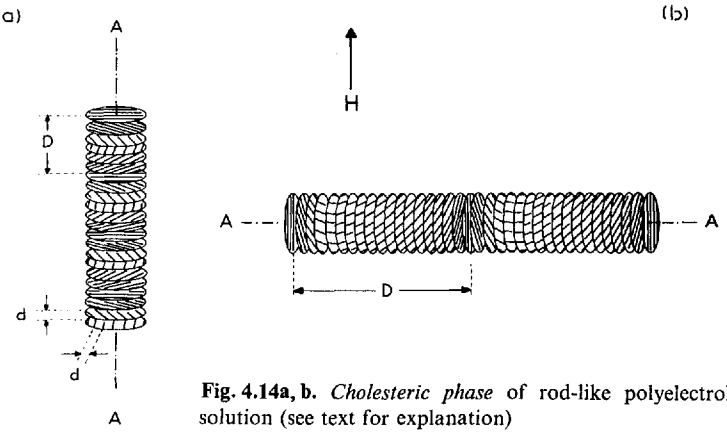

Fig. 4.14a, b. *Cholesteric phase* of rod-like polyelectrolytes in aqueous solution (see text for explanation)

rearranges, D increases and diverges at a critical field H_c, given [4.85] by

$$H_c = \frac{\pi^2}{2D_0}\left(\frac{K_2 \cdot l_0}{\Delta\chi_0 LN}\right)^{1/2}$$

using the symbols introduced in Sect. 4.3.1; D_0 is the optical periodicity in zero field and K_2 is Frank's elastic constant for twist deformation, which can be measured through H_c.

In thin samples with dominating wall effects the cholesteric axes can be forced to maintain certain directions with respect to the magnetic field. Since magnetic orientation of the cholesteric as a whole is thus prevented, K_2 or other elastic constants can eventually be measured even for molecules with $\Delta\chi < 0$.

The magnetic field is thus useful in several ways: to determine the sign of the diamagnetic anisotropy of the molecules in the ordered phase; to deduce information about the molecular order by observing the magnetic alignment and deformation behaviour under various boundary conditions, to determine elastic constants and to keep a sample macroscopically aligned. For example, the cholesteric solutions of fd belong to case (b), Fig. 4.14 [4.149]: the cholesteric axes orient perpendicular to the magnetic field ($\Delta\chi > 0$) in agreement with the observed [4.3, 5, 92, 148] tendency of the individual virus to orient along H. Because of the large diamagnetic anisotropy [4.92] and the small twist elastic constant K_2 ($\sim 10^{-8}$ dyn), the critical field for untwisting turns out to be small, amounting only to ~ 0.8 T for the sample in Fig. 4.13a [4.149]. This is of practical importance because the fully oriented ("forced") nematic state above H_c can be easily studied with a superconducting magnet.

As mentioned earlier, DNA and other double and triple helical *nucleic acids* – unlike bacteriophages and normal liquid crystals – orient perpendicular to H ($\Delta\chi < 0$). Long-range order and magnetic field effects in concentrated polyelectrolytic solutions of these molecules have been investigated by *Jizuka* et

al. [4.152–155] and by *Sénéchal* et al. [4.3, 4]. The first group studied viscous high molecular weight samples in relatively weak fields (<2.5 T) using magnetic birefringence, linear and circular dichroism, light-scattering and x-ray diffraction. The other group prepared almost rod-like fragments not much longer than the persistence length and obtained fairly liquid samples with better developed order, avoiding the chain entanglements; they used orienting fields up to 18.5 T and measured birefringence, small-angle neutron scattering and light diffraction. The observed critical concentrations are typically around 10 % w/w, which is an order of magnitude higher than for the bacteriophages, because for the semiflexible nucleic acids the length scale controlling the Onsager transition, given by twice the persistence length [4.141], is about an order of magnitude smaller (Sect. 4.3.2a) than the length of the rod-like phage. The short-range order turns out to be similar to that of the phages described above, but with much smaller mean next-neighbour distances (~ 4.7 nm) and thinner ionic cloud according to the higher concentration. The long-range periodicity is much shorter and best measured by Bragg diffraction of laser light (Fig. 4.15). For weak boundary conditions, the periodicity aligns parallel to a strong magnetic field just as expected for case (a) in Fig. 4.14.

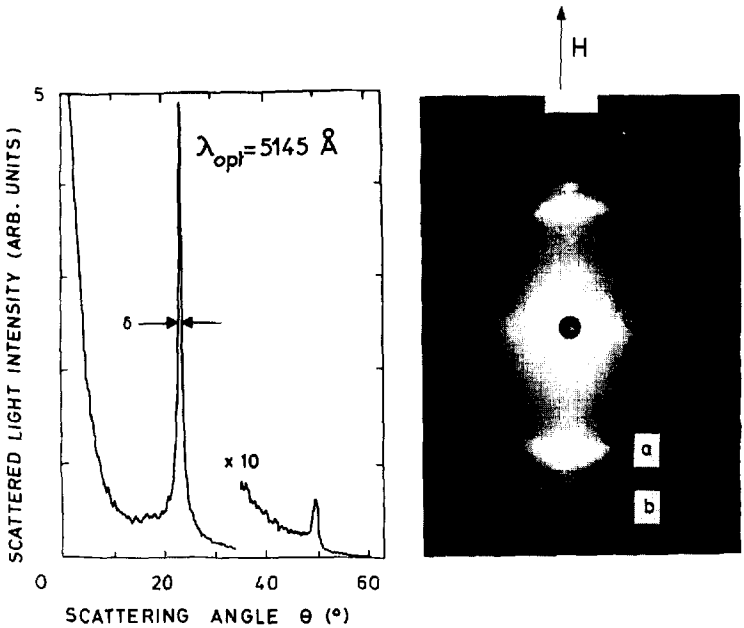

Fig. 4.15. A periodicity of long wavelength and very long coherence length apparently exists in aqueous solutions of semiflexible fragments of nucleic acids, amounting to 1.20 μm for Poly *A* · Poly *U* of mean molecular length ~ 1700 nm, concentration ~ 140 mg/ml, 4×10^{-3} M NaCl, $T = 20$ °C, cell thickness 0.1 cm. It gives rise to the sharp diffraction of visible light and is oriented parallel to a strong magnetic field (13 T). (*a*) $\lambda = 482.5$ nm, (*b*) $\lambda = 632.8$ nm [4.4]

Under strong boundary conditions, with magnetic field normal to the axis of the long period, *Jizuka* observed a magnetic field dependent increase of the long period, but a critical field could not be found. All the information quoted so far is consistent with a classical cholesteric lyotropic structure [4.154]. However, *Sénéchal* et al. [4.4] found that both the *Cotton-Mouton constant* and the high field *saturation birefringence are too small* to be accounted for by domain rotation and full high field alignment, respectively, of an ideal cholesteric. They suggested a cylindrical multishell model which is consistent with most of the data, but there is also agreement with a 3-dimensional twisted structure like *Robinson*'s spherolites [4.139].

In the examples discussed above, *repulsive* electrostatic long-range forces were important. It has been mentioned [4.4, 146, 147, 149, 150] that a small contribution of *attractive* forces due to electronic or ionic fluctuations cannot generally be neglected. In our view, the existence of such a force is the only reason for the twist between helical molecules at these large intermolecular distances.

II) Liquid Crystalline Polymer Solutions

Some of the concentrated polyelectrolytes treated in the last section are ("lyotropic") liquid crystals; they therefore essentially belong under this heading here. However, we want to distinguish between systems dominated by intermolecular long-range electrostatic repulsion and more concentrated systems, usually in organic solvents, where more specific steric short-range interactions between the molecules or their chemical side groups also come into play. The macroscopic properties of these two classes of liquid crystalline polymers are often hardly distinguishable.

It is well known that concentrated solutions of some polypeptides can be nematic or cholesteric (with typical radial molecular separations of the order of 1–2 nm) when the solvent favours a rigid α-helical conformation of the peptide backbone. The long-range orientational correlation then implies strong magnetic orientability even in moderate fields. The presumably first observation of magnetic orientation in such systems was in 1967; *Sobajima* [4.91] reported a strongly anisotropic motion of methylene chloride molecules as *solvent* for *poly-γ-benzyl-L-glutamate* (PBLG), deduced from high-resolution 1.4 T nuclear magnetic resonance. (No NMR signal from the polymer itself could be observed because of the strongly restricted segmental motion in the nematic phase, implying very broad polymer NMR lines.) Solvent molecules couple their orientation to that of the polypeptides. From the very long build up time ($\sim$100 min) of the solvent motional anisotropy after switching on the magnetic field, a slow reorientation of the α helices parallel to H was deduced. The orientation was confirmed by x-ray patterns of dry PBLG films prepared from the liquid crystalline state oriented in the magnetic field (Sect. 4.4). Sobajima's ideas were extended to other solvents and important information about the structure of the α helix was thus obtained, mainly by *Samulski* and coworkers [4.158–161].

An attempt to interpret the magnetic orientation in terms of diamagnetic anisotropies of the polymer constitutents was made in 1971/72: *Jizuka* and *Miyata* et al. [4.162–164] reported orientation perpendicular to H of the cholesteric helices of PBLG and magnetic untwisting. Similar but weaker effects were found in poly-γ-ethyl-*L*-glutamate (PELG) which contains no aromatic ring group; the authors concluded that besides the benzyl group the α-helical backbone is also diamagnetically anisotropic [4.165]. Interestingly, the observation of an overall orientation of PBLG *parallel* to the magnetic field excluded the existence of any side chain conformation in PBLG with the aromatic planes perpendicular or nearly perpendicular to the α-helical backbone. (Even any free rotation of the aromatic planes around an axis perpendicular to the backbone seems unlikely. In all these cases the intrinsic anisotropy of the backbone would be overcompensated by the mean side group anisotropy and an overall orientation of PBLG *perpendicular* to H should occur.) The observed *parallel* magnetic orientation is consistent with a recent model for the side chain conformation proposed by *Samulski* based on NMR data from magnetically oriented PBLG [4.166]. In addition these data give some evidence for interchain intercalation of the benzyl groups in liquid crystalline solutions of PBLG. *Jizuka* [4.167] and *Tohyama* and *Miyata* [4.82] gave $\Delta\chi$ values per α-helical peptide bond (Sect. 4.2), the latter deduced from direct measurements of the macroscopic magnetic torque on a previously oriented PBLG sample tilted 45° from the field direction. *Guha-Shridhar* et al. [4.168] measured the diamagnetic anisotropy of nematic PBLG with a magnetometer; their $\Delta\chi$ values led to the determination of the three principal elastic constants of lyotropic PBLG from optical observations of magnetic untwisting and from birefringence measurements mainly by *DuPré* and co-workers [4.168, 169]. From NMR of the weakly oriented solvent (H_2O), *Finer* and *Darke* [4.170] concluded that also the α-helical poly-L-lysine hydrobromide can be oriented in moderate magnetic fields.

The appearance of liquid crystalline phases in all of the polymer solutions discussed above is essentially due to the high rigidity of the polymeric backbone and intermolecular interactions ocurring at high concentrations. *Grossberg* et al. recently described the interesting idea that also flexible polymers at any dilution could be liquid crystalline: if the polymer contains rod-like so-called mesogenic groups (which as monomers would form a neat liquid crystal) and flexible spacers (Fig. 4.8), each individual polymer chain could collapse into a liquid crystalline globule at sufficiently small temperatures and favourable solvent conditions. Small globules forming at intermediate chain lengths should be very anisotropic, whereas large globules at high molecular weights should become isotropic [4.141]. A large number of such polymers has been synthesised in recent years and many display liquid crystallinity (*thermo*tropism) in the *melt* [4.171–173] (see the following section). Anisotropic globules in solution, clearly detectable by Cotton-Mouton experiments at different molecular weights, have not been found so far [4.112, 174].

III) Isotropic and Liquid Crystalline Polymer Melts

We now consider polymeric liquids *without solvent*. Much of the effort in polymer physics is related to studies of the *conformation of individual polymer chains* and their *correlation with neighbouring chains* in the liquid, amorphous and, more recently, liquid crystalline states.

As in the previous sections, strong magnetic fields are useful here mainly in two respects: to detect (small) orientational correlations of segments in the disordered melts via the Cotton-Mouton effect and, for highly correlated liquid crystalline systems, to produce strong orientation. In the latter case it should be possible to observe many of the magnetic field effects known for low molecular weight liquid crystals, but the field strength needed to produce the effects on a reasonable time scale could be substantially higher due to the generally elevated viscosities of the polymeric systems.

The local order of chains in the amorphous state is a debatable topic. Many contradictory models have been developed in the past; the one extreme *(Random-Coil model)* assumes a totally random configuration of the chain in the amorphous state as in the melt, just like the configuration in dilute solution; the other *(Bundle model)* predicts a short-range parallel order of the chains extending over some 1 to 10 nm [4.175]. Various techniques have been applied to solve this problem [4.108 and references therein]. Obviously magnetic orientation studies carried out directly in the amorphous state are of very limited significance because of the restricted freedom of any segments or bundles to rotate under field. There are, however, generally precursors of orientational correlations in the liquid state when cooled towards the transition temperature. These pretransitional effects are well known in liquid crystals above the isotropic to nematic transition (Sect. 4.3.3a). It can thus be expected that the existence of locally parallel chains in the amorphous state should be evident by a typical increase of the Cotton-Mouton constant when approaching the glass temperature T_G from above.

No such increase was found in melts of polystyrene [4.107, 176]. Above T_G the Cotton-Mouton constant stayed at an essentially temperature-independent small value which agrees well with the rotational isomeric state model of chains in the melt [4.107]. Below T_G CM is about 4 times smaller. This has been interpreted as a random coil conformation with high backbone flexibility and restricted but finite side group mobility in the amorphous state [4.107].

Extended Cotton-Mouton experiments have been carried out on melts of short *n-alcane chains* and *polyethylene* (Fig. 4.4a) [4.107, 108, 177]. A comparison of the results with experimental Cotton-Mouton constants from alcanes in solution demonstrates the existence of some short-range correlations in these melts. *Champion* et al. [4.177] pointed out difficulties in interpreting the data solely in terms of intermolecular correlations. However, CM shows a strong increase with decreasing temperature which coincides with the pretransitional $(T - T^*)^{-1}$ behaviour of liquid crystals. Since T^* turned out to be nearly

independent of the molecular weight, the existence of pretransitional correlations of trans-segments has been proposed [4.107, 108].

During the last years, liquid crystalline phases were discovered in melts of a number of special polymers. As mentioned in Sect. 4.3.2a, b, Subsection II, their monomers contain a rigid "*mesogenic*" *group* located in the main chain (Fig. 4.8) or in a side group and are linked by flexible spacers. By an appropriate choice of mesogenic group and spacer the temperature range of the liquid-crystalline phase(s) could be made substantial (some 50–100 °C) and kept well below temperatures of chemical decomposition. Thus these polymers became interesting in several respects. For example, an academic question concerns the microscopic structural order which results from the competing effects of anisotropic interactions between mesogenic segments and the intrinsic tendency of the polymer chain to avoid extended configurations. Elastic properties should differ from those of low molecular weight liquid crystals. Potential industrial applications range from the possible production of strongly oriented high modulus polymer fibres to special optical coatings, for example obtained by freezing a cholesteric texture in a polymer film. Several reviews have appeared recently [4.171–173].

Magnetic orientation in nematic phases of various of these polymers has been studied in several laboratories since 1980 [4.174, 178–185]. For some of the polymers with mesogenic groups in the main chain strong orientation along H of at least the mesogenic groups was observed in fields around 1 T. This was clearly demonstrated by x-ray diffraction (Fig. 4.21 below) [4.178, 183, 185], NMR [4.182] and measurements of the diamagnetic anisotropy [4.180, 184]. Substantial new information about the structure of the nematic phases was thus obtained. There appears to be, however, a critical field below which no orientation occurs and, as do speed and final degree of alignment, it depends on the polymer's properties such as molecular weight, lenght of the spacer group and flexibility. Cholesteric polymers could not be aligned even at 12 T, underlining the importance of stronger fields for the study of a wider variety of these polymers. Interestingly, the experiments mentioned above revealed orientational order parameters of the mesogenic main-chain groups in the nematic state of about 0.6 to 0.8, which is some 50 % to 100 % higher than values for low molecular weight nematics. The property – promising for applications – can possibly be related to the particular isotropic-nematic transition behaviour found [4.182] in some of the polyesters. As outlined in Fig. 4.16, the polymer exhibits a pretransitional increase of the Cotton-Mouton constant $(T-T^*)^{-1}$ like classical liquid crystals such as PAA, but the difference between T^* and the real transition temperature T_c (clearing point) is much larger. This combined with a high value of the latent heat at T_c indicates that the polymeric transition is "much more first order"; following the Landau-de Gennes description of the transition it also leads to the prediction of a high-order parameter in the nematic phase. The values thus deduced agree with those derived from NMR [4.181, 182].

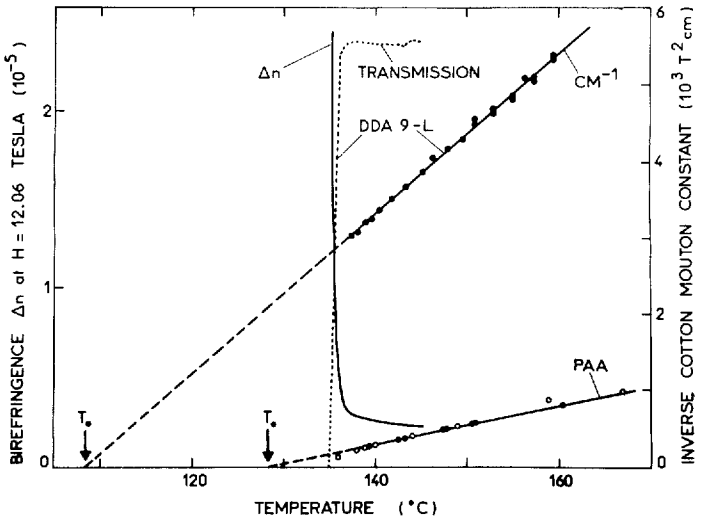

Fig. 4.16. The pre-transitional effects of a melt of the polyester DDA 9-L (Fig. 4.8) in comparison to a classical liquid crystal, *p*-azoxy-anisole ($CH_3-O-\langle O \rangle-N(\downarrow O)=N-\langle O \rangle-O-CH_3$). Above the isotropic-nematic transition temperature T_c ($\simeq 132\,°C$ for PAA and $\simeq 135\,°C$ for DDA 9-L) the Cotton-Mouton constant (● data [4.182]; ○ data from [4.187]) of both samples is proportional to $T-T^*)^{-1}$ over an extended temperature range. T^* is evaluated by linear extrapolation and T_c determined by the onset of strong turbidity, resulting in a sudden drop of optical transmission (···) and by the divergence of the birefringence in a constant magnetic field (——). $T_c - T^*$ is much larger for the polymer ($\sim 27\,°C$) than for PAA ($\sim 3.4°$). Similarly the latent heat of the polymer at the transition exceeds that of PAA by about 5.4 times. Using the magnetic birefringence and calorimetric data the absolute values and temperature variation of the order parameter at *both* sides of the transition can be calculated using the *Landau-de Gennes* theory [4.85, 105]. The values thus predicted for the nematic phase of the polymer agree with the large experimental values cited in the text [4.182]

4.3.3 Classical Liquid Crystals

A large number of various anisometric – rod-like or disc-like – small molecules exhibit liquid phases with some orientational and translational long-range order at temperatures between the crystalline and isotropic liquid state; therefore they are called thermotropic liquid crystals. An example cited above (Fig. 4.16) is PAA. With molecular diamagnetic anisotropies typically like benzene and large correlation lengths in the liquid crystalline phases, they show many magnetic orientation effects, sometimes in fields far below 1 T which have been extensively described [4.1, 85, 157, 186]. Since this chapter deals mainly with *macro*-molecules, only some recent experiments involving high fields will be mentioned.

a) Pretransitional Effects in the Isotropic Phase

When the isotropic phase of a liquid crystal is cooled towards the nematic transition, increasing pretransitional orientational correlations occur

very similar to the spin correlations in a paramagnetic substance above the Curie temperature. They result in an enhanced magnetic birefringence, observed by *Tsvetkov* already in 1944 [4.187]. *De Gennes* [4.85] pointed out that in Landau's mean field approximation, the Cotton-Mouton constant which is a measure of the local order parameter should, like the Curie-Weiss susceptibility, be proportional to $(T-T^*)^{-1}$, where T^* is the temperature of a *second*-order transition. This behaviour and small deviations from it occurring close ($\sim 2\,^\circ$C) to the thermodynamically manifested first-order isotropic-nematic transition temperature T_c were accurately measured by *Stinson* and *Litster* in 1970 [4.188]; T^* is about 1° below T_c, therefore the isotropic-nematic transition is sometimes called a "weakly" first-order transition. Later birefringence measurements in high fields enabled the range of the pretransitional effects to be determined on the high-temperature side where CM is small [4.189, 190]. Also $T_c - T^*$ could be evaluated more precisely and the deviations of the order parameter from the $(T-T^*)^{-1}$ behaviour closer (a few tenths of a degree) to T_c [4.191] were evaluated. Even in the vicinity of T_c, CM exceeds the high temperature and solution values only by about 2 orders of magnitude. In terms of the number N_1 of correlated molecules (defined in Sect. 3.1) this means that the orientational correlation is still fairly short range ($N_1 \sim 10^2$). Thus the degree of orientation ($\sim N_1 \Delta\chi H^2/kT$) remains small even in a field of 10 T. This is also reflected by the strictly linear relationship between Δn and H^2 found by *Poggi* and co-workers over all field strengths investigated (< 13.5 T), and by the high field value of $\Delta n\,(\sim 10^{-4})$ which is small compared to Δn values of completely oriented nematics ($\Delta n_{sat} \sim 10^{-1}$). In contrast to these results, *Keyes* and *Shane* [4.192] recently reported a linear H dependence of $(\Delta n/H^2)$ up to 10 T particulary pronounced near T_c. No explanation has yet been offered for this experimental disagreement.

It is obvious from simple thermodynamic considerations that T_c *itself should depend on the magnetic field strength*: since in, say, 10 T the isotropic and nematic phases are very weakly and strongly oriented, respectively, the relative shift of T_c is of the order $\Delta\chi H^2/Q$, with $\Delta\chi$ being the diamagnetic anisotropy of the nematic phase and Q the latent heat [4.193]. This relation has been verified experimentally by *Rosenblatt* [4.193] in strong magnetic fields; the absolute shift amounts to only 5×10^{-3} °C at 15 T.

b) Orientational Fluctuations in the Nematic Phase

In the nematic phase the orientational correlation lengths are macroscopic. Hence almost completely oriented samples form spontaneously in small containers with walls treated so as to impose a direction to those molecules in contact with the wall. The intrinsic (zero-field) birefringence of such samples is very large, typically of the order of $\Delta n \sim 10^{-1}$. There are, however, thermal fluctuations of the direction of the long axes of the molecules around the average (macroscopic) axis of alignment. Their amplitudes can be slightly reduced in a strong magnetic field. The corresponding small increase of birefringence Δ

(typically some 10^{-5} at 10 T) was theoretically predicted by *de Gennes* [4.85] and observed by *Poggi* and *Filippini* [4.194]. In this case Δ is proportional to the magnetic field, essentially because fluctuations with wavelengths longer than the magnetic correlation length ξ are quenched [4.85]. This ξ is a characteristic length resulting from a balance between magnetic and elastic torques, roughly corresponding to the shortest distance between a molecule clamped in a given direction and molecules parallel to the magnetic field. Depending on the geometry (i) it equals

$$\xi = (K_i/\Delta\chi)^{\frac{1}{2}} H^{-1},$$

with K_i the elastic constants for splay ($i=1$), twist ($i=2$) or bend ($i=3$), respectively. Since for small changes in ξ the birefringence increment Δ must be proportional to ξ^{-1}, it follows that $\Delta \sim H$. *Malraison* et al. [4.195, 196] extended *de Gennes'* theory [4.85], originally developed for a mean elastic constant, to the more general case of different splay, twist and bend elastic constants. They also measured Δ/H over the complete nematic temperature range. Including the temperature-dependent values of the elastic constants determined by other techniques they found good agreement between their theory and experiments, except for temperatures near the nematic isotropic transition. Because of the naturally limited sample length and the small Δ values, such experiments necessitate the combined application of strong fields and sensitive birefringence techniques.

The orientational order parameter of nematic liquid crystals has been estimated from measurements of the anisotropy of the diamagnetic susceptibility of a nematic glass produced by quenching a liquid sample in a strong magnetic field [4.197].

c) Untwisting in the Cholesteric Phase

As mentioned above, the coherence length ξ is proportional to H^{-1}. Transitions of *nematic* into aligned phases usually occur at a critical magnetic field H_c above which $\xi(H)$ is smaller than a typical dimension of the sample, for example the distance between the confining glass plates which can be around 100 μ. With common values for K_i and $\Delta\chi$, H_c ranges well below or around 1 T. In *cholesterics*, however, the equivalent typical dimension is the pitch. Because the pitch in normal cholesterics is generally comparable to optical wavelengths or even smaller, the critical fields for untwisting are somewhat above presently available field strengths. Therefore magnetic untwisting has been observed so far only in special cholesterics with large pitches, such as the α-helical polypeptides, concentrated solutions of virus (Sect. 4.3.2b, Subsection II) or solutions of cholesterics in nematics [4.1, 85, 115]. Certainly, also some of the other magnetic field effects often discussed could become observable in very strong fields (~ 30 T) for a number of cholesteric materials, depending on the sign of $\Delta\chi$, the size of $\Delta\chi/K_i$ or the influence of the wall.

4.3.4 Membranes and Micelles

a) Background

We now turn to so-called amphiphilic molecules, which consist of a polar head group soluble in water (hydrophilic) and an aliphatic tail (hydrophobic). Therefore, when suspended in water at low concentration, they form organised aggregates such as double layers (membranes), vesicles or micelles in order to maximize both exposure of head groups to water and mutual contact of tails. Similarly inverted structures might occur in oil. In oil/water mixtures the amphiphiles tend to cover the interface, thus acting as detergents. At higher concentrations the aggregates can form various ordered or sometimes liquid crystalline phases, depending on chemical composition, solvents, presence of ions or of other molecules like alcohols, temperature, etc. In contrast to the polymeric systems, both the number of molecules contained in these objects (corresponding to their molecular weight) as well as their shape are often variable and frequently not known. This and their multicomponent nature usually make structural investigations of these systems sometimes more complex than for lyotropic polymers or thermotropic liquid crystals. Organised biological membranes containing proteins in the amphiphilic layer are treated separately in Sect. 4.3.4c.

b) Artificial Multilayers and Micelles

I) Expected Magnetic Field Effects

The number of correlated molecules within such systems can be enormous and substantial magnetic orientation effects are expected, although quite often groups with large $\Delta\chi$ values like aromatics are missing. A major contribution to $\Delta\chi$ might originate from the more or less ordered hydrocarbons in the hydrophobic layer. Some values are compared in Table 4.3. The uppermost value results from a simple estimate of the difference between normal and planar χ values for a sheet of normally oriented all-trans $(CH_2)_{18}$ chains using the C−C

Table 4.3. Diamagnetic anisotropy[a] of oriented hydrocarbon systems and bilayer membranes

C_{18}	−6.5 (±25%)	Estimated from C−C bond anisotropy
Partially crystalline polyethylene $(CH_2)_x$	−1	[4.198]
Crystalline stearic acid $CH_3(CH_2)_{16}COOH$	−9.7 (±20%)	[4.64]
Crystalline dipalmithoyl--L-α-lecithin	−9	[4.198]
Egg lecithin membranes	−0.27	[4.199]

[a] Volumetric susceptibilities in 10^{-8} cgs units. The densities of all systems mentioned are very close to 1 g/cm^3

bond anisotropies (neglecting C−H) cited in Sect. 4.2. It is the same order of magnitude as experimental values from stearic acid crystals. These values should be considered as upper limits for a pure hydrocarbon layer. Orientational disorder lowers $\Delta\chi$ substantially, as can be seen by comparison with partially crystalline polyethylene containing disordered amorphous regions. It is seen from the sign of $\Delta\chi$ that individual extended hydrocarbon molecules tend to align perpendicular to H and hence the plane of a layer or membrane aligns parallel to H. Dipalmitoyl lecithin (DPL), a molecule consisting of two hydrocarbon chains and a polar head group, aggregates in water into bilayer membranes which are widely used as models for biological membranes. *In crystals* of DPL, bilayers are formed with parallel hydrocarbon molecules; the elongated head groups are roughly perpendicular to the hydrocabon long axis and all point in a given direction in the bilayer plane. Thus the crystals are biaxial. From the observed *biaxial* orientation behaviour of such crystals in a magnetic field, *Sakurai* et al. [4.198] estimated the normal-planar anisotropy of DPL bilayers (Table 4.3) and deduced that the head group has a remarkable diamagnetic anisotropy. They did not evaluate the head group anisotropy quantitatively, however. Interestingly, the normal-tangential anisotropy of an egg lecithin membrane, as derived from the slow alignment along H of large elongated vesicles, turned out to be much smaller than the above values derived from crystals [4.199]. This can be accounted for primarily by the substantial molecular disorder in the egg lecithin membranes, which consist of a mixture of various different amphiphilic molecules. The egg lecithin anisotropy is more than two orders of magnitude smaller than the usual anisotropy in liquid crystals ($\Delta\chi \sim$ some 10^{-7}).

Nevertheless strong orientation of such hydrocarbon systems must occur in high fields. Using, for example, as typical values $\Delta\chi = 2 \times 10^{-8}$, a layer thickness d of 5 nm, $H = 20$ T, $T = 300$ K, orientation would become substantial (i.e. $\Delta\chi H^2 a L^2/kT > 1$) for flat rigid layers with area L^2 larger than 100×100 nm^2, or for correspondingly smaller multilayer stacks. Ordered rigid objects larger than this are obviously quite common in many emulsions or biological systems. In addition, the presence of aromatic (head) groups or protein might substantially enhance $\Delta\chi$ numerically and even change its sign. Magnetic orientation and birefringence of rigid non-interacting objects in suspension such as disk-, tube- or cigar-shaped vesicles can be described straightforwardly by the equations in Sect. 4.3.1. All one needs to do is to calculate the effective anisotropies of each object by geometrical summing over molecular anisotropies or over the effective values per unit area. In this way a magnetic birefringence experiment yields *information about the anisotropic shape of the object*, if the molecular quantities are known, or vice versa. In case the refractive index inside the object differs from the solvent index (for example, in oil-detergent-water systems), shape birefringence might become important compared with the intrinsic birefringence of the anisotropic shell [4.200].

Spherical vesicles or micelles obviously do not orient. However, the possibility of magnetic deformation into elongated ellipsoids has been theoreti-

cally discussed by *Helfrich* [4.201, 202]. From a balance of the magnetic and elastic torque on the surface elements, he derived that the relative deformation should be $\Delta r/r = \Delta\chi H^2 a r^2/12\kappa$ for small deformations; r is the unperturbed radius of the object and κ the bending elastic modulus of the shell. As defined by the elastic energy $\varepsilon = \kappa/2r^2$ per surface element for an isotropic elastic medium, κ is related to the bulk elastic constant K by $\kappa = Ka$. The magnetic birefringence due to deformation is of the order of

$$\Delta n \sim \Delta n_{\text{sat}} \cdot \frac{\Delta r}{r}$$

with typically $\Delta\chi = 2 \times 10^{-8}$, $H = 20$ T, $a = 5$ nm, $r = 25$ nm, $\Delta n_{\text{sat}} \sim 10^{-4}$ at a volume fraction of 10^{-2} and $\kappa = 10^{-13}$ erg for liquid crystals we estimate $\Delta r/r \sim 2 \times 10^{-3}$ and $\Delta n \sim 2 \times 10^{-7}$. Thus, though the deformation is small, it should be detectable in strong magnetic fields and *the bending elasticity of the microscopic objects can be directly determined*, if κ is not too large.

So far we have treated rigid particles and have omitted thermal fluctuations of shape. These are important when the elastic energy εr^2 in the sphere becomes smaller than kT, hence for $\kappa \lesssim kT$. This situation possibly occurs for example in thin layers of detergent molecules in the presence of alcohols which seem to reduce the longe-range order [4.200]. In analogy to the persistence length in polymers (Sect. 4.3.1), *de Gennes* [4.200] introduced the idea of a persistence area ξ^2. In this description the flexible layer would be replaced by rigid plates of length ξ linked by ideally flexible joints. Here ξ should be of the order $\xi = e \exp(2\pi\kappa/kT)$, with e being a molecular length scale, for example the diameter of an amphiphilic molecule [4.200]. Therefore the number of molecules contained in a persistence area is about ξ^2/e^2 and magnetic orientation and the Cotton-Mouton constant are expected to be proportional to ξ^2/e^2; in fact $\xi^2/e^2 \simeq N$, as defined in Sect. 4.3.1 [4.203]. This concept, which has not been verified experimentally yet, is interesting because of the sensitive (exponential) dependence of magnetic orientability on K. It can be applied to any semiflexible layer system, i.e. if the extension of the objects is much larger than ζ. In this way κ could be determined also for very flexible vesicles or micelles, for which $\xi \ll r$. The region of cross-over ($\xi \sim r$) between flexible and rigid ($\xi \gg r$) vesicles is more complex and the magnetic orientation and deformation behaviour has not yet been worked out.

In the preceding section we considered the membrane as a layer with maximal symmetry, the symmetry axis being identical to the normal of the plane. However, bilayer membranes often have a complicated internal structure; phases are known involving tilting of the molecular long axes with respect to the normal (Fig. 4.17) or an in-plane orientation of the head groups. These phases are biaxial at least on a local scale and a large membrane can be considered as a planar ensemble of biaxial domains. Thus even if magnetic alignment of the membrane as a whole is prevented, for example in a multilayer sandwich-type sample confined between planar glass plates, magnetic orientation of the

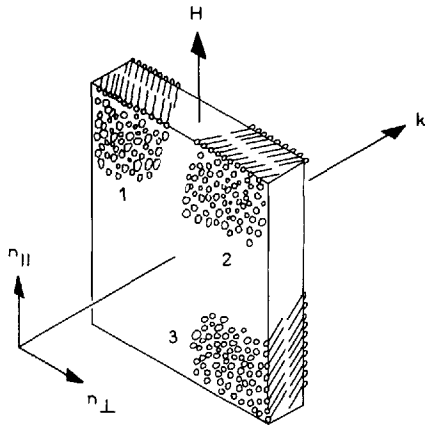

Fig. 4.17. In a membrane containing domains of tilted molecules, magnetic orientation could occur due to in-plane rotation of domains, e.g. if the membrane plane is fixed by wall effects parallel to H, domains *1* and *2*, (*3*), have favourable (unfavourable) orientation; hence domain 3 rotates around $\boldsymbol{k}$ by 90° in a magnetic field sufficiently strong to bring the molecular long axes normal to H. This results in a birefringence $\Delta n = n_{\parallel} - n_{\perp}$. The orientation mechanism was first proposed by *Gaffney* and *McConnel* [4.204]. In-plane anisotropy can also result from a cooperative tilt of anisotropic head groups [4.205]

domains could occur as depicted in Fig. 4.17. The correlation lengths (defining the domain size) for the tilt of tails and heads, respectively, need not necessarily be related; they might also differ from ξ.

Thus quite a number of interesting magnetic field effects can be expected in emulsions of amphiphilic molecules.

II) Experimental Observations

We treat magnetic orientation studies of detergent containing systems and artificial membranes (phospholipid-layers) in two separate sections, because the latter are related to biological membranes.

In detergent-containing systems, magnetic orientation was first realized by *Lawson* and *Flautt* in 1967 [4.206]. Mixtures of typically 50 % water (D_2O), 42 % soap (sodium decyl sulphonate, SDS), 4% alcohol and 4% salt (Na_2SO_4) showed deuterium NMR spectra much like those in a magnetically oriented nematic liquid crystal. Since many such systems at elevated concentrations display some liquid-crystal like order, the ease of magnetic orientation of these phases in low fields has been frequently used since [4.207–211 and references therein]. This was most important for structural aspects, for example to decide whether the anisotropic objects forming the liquid crystalline phase were either disc-like or rod-like [4.207, 209]. Unfortunately a somewhat confusing classification and nomenclature was introduced: systems with alignment of the rotational symmetry axis of the aggregates parallel (or perpendicular) to H have been called "type I" (or "type II") or "positive" ("negative") diamagnetic anisotropy. Type I (type II) was usually associated with rod-like (disc-like) aggregates, which is obviously true only for layers with negative normal-tangential anisotropy such as the hydrocarbon-layers in Table 4.3. The reverse situation of positive normal-tangential anisotropy can easily occur when the molecules contain oriented aromatic groups. Another aspect concerned the

possibility of using these phases as oriented matrices *for aligning a wide variety of small host molecules* as to whether they were soluble in an aqueous or aliphatic milieu. Periodic textures were observed to occur in a magnetic field and interpreted by an orientation-induced flow process [4.210]. It is noteworthy that addition of small polymer-coated ferromagnetic particles ("ferrofluids") to the emulsion seems to enable magnetic orientation [4.212] and deformation [4.213] already in very weak fields.

A substantial amount of intermolecular order might persist in detergent-containing systems even under conditions where turbidity is essentially absent and no liquid crystallinity exists. For example, soap molecules in pure water with or without salt form micelles which can adopt various sizes and shapes; oil-water-soap emulsions often turn transparent when a certain amount of alcohol is added, and are then called microemulsions. Structural investigations of such phases are important for the development of specific applications of soap. *Porte* and co-workers [4.214–217] studied the polymorphism and interactions of micelles of different soaps in dilute aqueous solution by high field magnetic birefringence. The soap molecules carried aromatic groups in the head region to enhance both diamagnetic and optic anisotropy. These measurements clearly demonstrated the existence of four distinct concentration regimes for sodium octyl benzene sulphonate in water. They have been interpreted in terms of *magnetic orientation of* free monomers and *more or less anisotropic micelles* [4.214, 215]. Possible contributions from other birefringence-producing mechanisms such as those outlined in (Sect. 4.3.4b, Subsection I) were not discussed. The experiments on cetylpyridium with NaBr in water are consistent with a worm-like model of fairly elongated micelles. Through a combination with light-scattering experiments a persistence length of about 20 nm at a micellar diameter of 6 nm was derived [4.216, 217].

Series of magnetic birefringence measurements were also performed on microemulsions [4.218]. Over a wide range in the phase diagram (of Na octylbenzene sulphonate, pentanol, decane and water) the Cotton-Mouton constant turned out to be small and consistent with an orientation of weakly anisotropic micelles, or of persistence areas, or with Helfrich's magnetic deformation mechanism. An extension of these measurements to monodisperse micelles at a series of calibrated radii, and eventually an independent determination of the yet unknown value of κ, should yield a better understanding of the behaviour of microemulsions in strong magnetic fields.

Large numbers of synthetic and natural lecithins or phospholipids in aqueous suspension spontaneously form bilayer structures (Fig. 4.17). They are widely studied as simple model structures (without proteins) for biological membranes. Many experiments are actually carried out on sandwich-like multibilayer stacks containing approximately equal amounts of lipid and water. Coplanar orientation of the bilayers is obtained between parallel glass plates; if more dilute emulsions are homogenised by ultrasound the bilayers form closed vesicles and samples of monobilayer vesicles with fairly narrow distribution of diameters can be prepared. Diameters might range from some 20 to 100 nm.

Under other conditions larger multibilayer "onion-like" vesicles are the most stable structure.

It was on oriented stacks of phospholipid bilayers that *Gaffney* and *McConnell* [4.204] in 1974 first found a direct magnetic field effect. They observed an anomalous spin label ESR signal for the planar orientation of H (Fig. 4.17). The ESR signal could not be fitted by any orientational distribution of the lipid molecules with rotational symmetry around an axis normal to the membrane. They proposed the mechanism of *in-plane rotation of tilted domains*, outlined in Fig. 4.17, which was consistent with the ESR results. Later, a small magnetic birefringence signal was observed [4.129] on multilayer stacks of egg lecithin and dimyristoyl lecithin, when the light beam pointed normal to the stack (Fig. 4.17). These data also agree with the above mechanism. Interpreted by a rotation of the tilted hydrocarbon chains and neglecting any anisotropy of the head, they would result in a mean domain size of the order of $100 \times 100\ \text{nm}^2$. However, a recent ESR study [4.219] on spin labels attached to the head group of dipalmitoyl lecithin provided evidence of a *cooperative rotation of the head groups* in a magnetic field. Thus the magnetic birefringence data should be reinterpreted including head group orientation and anisotropies; the latter could be estimated from bond anisotropies.

In Sect. 4.3.4b, Subsection I, was outlined that suspended vesicles should have more freedom than fixed membrane stacks to reorient in a strong magnetic field. The possibility of measuring elastic constants, orientation correlation lengths and small anisomeries as well as their relevance for biomagnetic effects make such studies an interesting topic in spite of their complexity. The actual knowledge is fairly scarce; we are aware of only two experiments.

Boroske and *Helfrich* [4.199] observed with a phase contrast microscope that large cigar-shaped ($\sim 30\ \mu\text{m}$ length and $\sim 10\ \mu\text{m}$ diameter) vesicles of egg lecithin slowly oriented parallel to a 1.5 T field. They deduced from the temporal sequence of the alignment the normal/tangential anisotropy of the volume susceptibility, which turned out to be rather small (Table 4.3). This can be explained by tilting, disordered lipid conformations or reorientations of tilted domains within the membrane. A magnetic deformation could not be found probably because of the use of *multi*layer membranes (large κ) and the difficulty of detecting small deformations with a microscope. High field birefringence experiments [4.6, 129, 220] were carried out on aqueous emulsions of dipalmitoyl lecithin, containing small (~ 60 nm) almost spherical bilayer vesicles and some larger onion-like multilayer vesicles of irregular shape. An electron microphotograph of such a sample (after drying on a substrate and staining) is shown in Fig. 4.18. Partial saturation of Δn was observed to occur in high magnetic fields, indicating that some of the larger aggregates can be completely oriented. Figure 4.18 shows the derivative of Δn with respect to H^2 measured at a fixed intermediate field strength by superimposing a small field modulation. It contains contributions from the small and large vesicles. Most pronounced changes can be seen at the pretransition and main transition, where the lipid chains transform with increasing temperature from an extended tilted to an

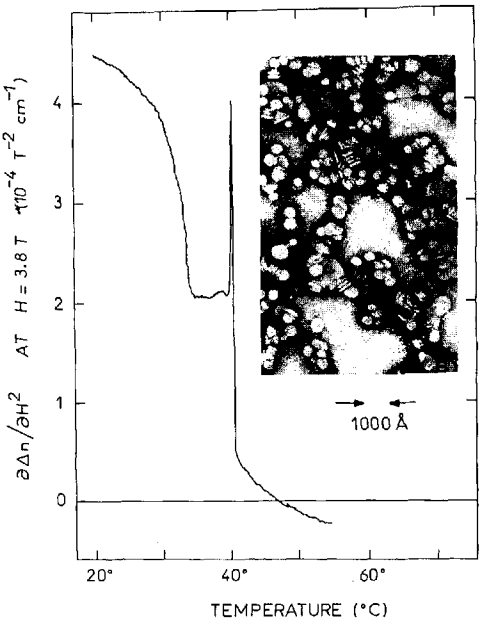

Fig. 4.18. Temperature dependence of the magnetic birefringence of suspensions of dipalmitoyl lecithin vesicles [$c = 20$ mg/ml, 5 mM $La(NO_3)_3$, $\lambda = 632.8$ nm, continuous variation of temperature at a rate of 0.5 K/min]. The magnetic birefringence suddenly changes at both the pretransition at 35 °C and the main transition at 41 °C of the lipid chains in the bilayer, so demonstrating the high sensitivity of this technique to detect transitions between phases of different lipid order [4.220].

extended non-tilted and to a disordered configuration. The magnetic anisotropy is related to the orientational order of the lipids. Since these transitions should also involve changes in orientational correlations, head group orientation, vesicles shape and κ, a quantitative interpretation of the detailed features of the data has not been made yet.

c) Organised Biological Membranes

Biological membranes consist of a phospholipid bilayer with various proteins embedded in or attached to it. The proteins control physicochemical and functional-biological properties of the membrane. Some proteins are known to cause structural changes within the neighbouring phospholipid bilayer, thereby influencing the bilayer's diamagnetic anisotropy; they can also contribute to the overall diamagnetic anisotropy of the biological membrane. In many biological systems large multilamellar arrays of biological membranes exist. It is therefore not surprising that already about 15 years ago full magnetic orientation in fields below 2 T was observed on outer *segments of retinal rods* [4.7] and *chloroplast*-containing cells of chlorella [4.88].

I) Outer Segments of Retinal Rods

The outer parts of retinal rods are cylindrical segments typically 50 μm long and 10 μm in diameter built up of a multilamellar stack of disc-shaped membranes. Membrane bilayers are perpendicular to the rod axis and consist to almost equal

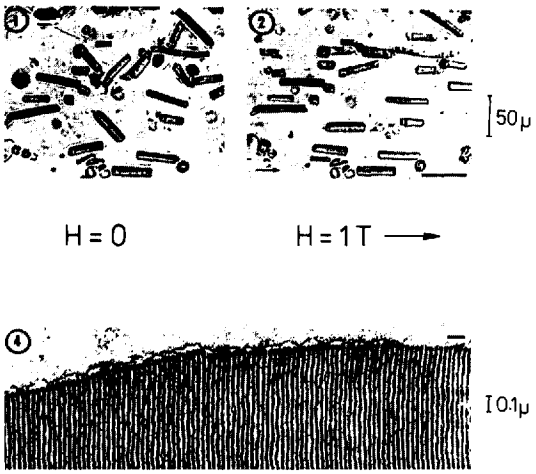

Fig. 4.19. Magnetic orientation of outer segments of retinal rods in suspension can be observed already at modest fields $\gtrsim 1.0$ T. Their large diamagnetic anisotropy is mainly due to the highly ordered arrangement of α-helical proteins in the membrane stacks [4.7]

amounts of lipid and protein; about 85 % of the protein mass is the visual pigment rhodopsin. The early optical observation [4.7] that in suspension these segments aligned parallel to a magnetic field of 1 T (Fig. 4.19) has stimulated a number of studies, resulting in important information about the structural order of the disc membranes. From the time course of the orientation after switching on the magnetic field, *Chagneux* and *Chalazonitis* determined the diamagnetic anisotropy $\Delta\chi_R$ of the segments [4.221]: $\Delta\chi_R$ is completely suppressed by CO_2 gas [4.222] and decreases by about 20 % upon bleaching with intense light [4.223].

A better understanding of the large segmental anisotropy $\Delta\chi_R$ in terms of phospholipid bilayer and protein (aromatic amino acids, retinal chromophore and α-helical polypeptide chain) was initiated by the theoretical work of *Hong* et al. [4.90]. More recent contributions are from *Chabre* and co-workers [4.224, 225] as well as *Becker* et al. [4.226]. The *phospholipid membrane* cannot be the major contributor to $\Delta\chi_R$ since this would imply an orientation of the segments *perpendicular* to H, as pointed out in Sect. 4.3.4a. Nevertheless, its contribution is not negligibly small [4.227]. A contribution of the aromatic *retinal chromophore* of rhodopsin can presumably be neglected [4.224, 226]; as indicated by linear dichroism measurements [4.226] this group strongly reorients on bleaching, which would necessitate a bleach *enhancement* of $\Delta\chi_R$ in contrast to the measured decrease of $\Delta\chi_R$ [5.223, 224]. The magnetic linear dichroism data [4.224, 226] also show that on the average, only one out of 61 *aromatic amino acid residues* per rhodopsin molecule has a non-random orientation; it is aligned with the aromatic plane parallel to the segmental long axis. Therefore the aromatic groups all together account for only at most 15 % of $\Delta\chi_R$ [4.224]. *Chabre* pointed out that the major contribution to $\Delta\chi_R$ may originate from the *α-helical (≈ 50 %) part* of the rhodopsin molecules; the α helices seem to be oriented normal to the disc membrane plane [4.224]. This was confirmed by the observation of a high linear infrared dichroism from the C=O-bonds in the α helix of magnetically

oriented segments [4.225]. Neutron small-angle scattering from oriented pellets, produced by sedimenting retinal segments in 1.7 T, has been used to determine which fraction of the rhodopsin molecule is embedded in the membrane and how it changes with bleaching [4.228]. Well-oriented samples for photochemical studies at low temperatures (77 K) could successfully be prepared only by quenching in a strong (17 T) magnetic field [4.229]. In this way disorienting effects due mainly to convection during cooling were overcome.

II) Systems Containing Chloroplasts

An important and rapidly developing field of biological and biophysical research concerns the molecular processes involved in the photosynthesis of plants. One particular structural aspect is the orientational order of the photosensitive molecules (chlorophyll) within the innercellular light-sensitive organelles, the chloroplasts. In 1971 *Geacintov* et al. [4.89] observed that the chlorophyll "*a*" fluorescence in a monocellular green alga (which contained only one chloroplast) was anisotropic in magnetic fields of 1.6 T. This is due to a strong alignment of the multilamellar disc-like chloroplast normal to H. A large number of mainly optical studies followed this observation, reviewed by *Hong* in 1976 [4.230] and theoretically described to some extent by *Knox* and *Davidovich* in 1978 [4.231]. We therefore restrict ourselves to a few remarks [4.230–243].

An attempt to explain the observed magnetic orientation of chloroplasts in terms of diamagnetic anisotropy of constituent molecules was made by *Geacintov* et al. From linear dichroism of rhodamin 6*G* attached to phospholipids they deduced that the membrane stacks orient normal to H; therefore the phospholipids contribute only weakly, if at all, to $\Delta\chi$. Besides some possible minor contribution from other lipids, carotenoid lipids, it is thus the proteins that determine $\Delta\chi$ [4.232]. The orientation relative to the membrane of various groups in the chlorophyll molecule (and their optical transition moments) has since been studied with many optical techniques mainly by *Breton* et al., though a satisfactory calculation of $\Delta\chi$ has not appeared yet. This might be partially due to uncertainties in the chloroplast's overall shape and to the variety of contributing molecular groups. Aromatic porphyrin rings of chlorophyll as well as aromatic tyrosines of the structural proteins tend to be perpendicular to the membrane plane, whereas α helices and carotenoid molecules are nearly in plane; other groups with unknown orientations possibly contribute to $\Delta\chi$ as well. Nevertheless, magnetic fields in the tesla range become a useful and easy tool for producing full alignment of chloroplast systems. Various studies of structural and optical aspects of photosynthesis have benefitted from this.

Neutron small-angle scattering by *Neugebauer* et al. [4.244] has shown that also bacterial chromatophores (planar pieces of purple membranes of the *Halobacterium halobium*) substantially orient in modest fields. As in retinal rods and chloroplasts, the membrane aligns normal to H. It was suggested by *Worcester* [4.79] that the ordered α helices of bacteriorhodopsin are responsible for the diamagnetic anisotropy of this system.

4.3.5 Other Biological Particles

Substantial progress in molecular biology is due to the knowledge of the atomic structure of biological particles like proteins as obtained mainly from x-ray work on crystalline samples. Unfortunately various bioparticles do not crystallise and different techniques (of comparably low structural resolution) have to be applied to gain information about their structure in a solution. Some techniques, for example NMR, ESR, Raman scattering or infrared absorption, are sensitive to local properties of single groups, others, like elastic light scattering, sedimentation and viscosity measurements, to the overall size and shape. In this section we wish to outline that magnetic birefringence and dichroism experiments, feasible even on small particles of modest $\Delta\chi$ in dilute solutions by using strong magnetic fields, can also yield *structural* information.

A *magnetic birefringence* experiment gives immediately the product $\Delta\chi \cdot \Delta\alpha$ for an isolated rigid particle (Sect. 4.3.1). Since measurements are usually carried out at wavelengths far from optical absorption bands, the birefringence originating from various anisotropic groups within the particle thus is determined by the anisotropies ($\Delta\alpha_i$) of these groups (species i), their relative orientation and their total number N_i per particle. To a good approximation it can be calculated by geometric summing

$$\Delta\alpha \cong \sum \Delta\alpha_i N_i f_i \,.$$

Here f_i can be considered as the average orientation factor for the groups of species i with respect to the particle's symmetry axis and $0 < f_i < 1$. An analogous relation holds for

$$\Delta_\chi \cong \sum \Delta\chi_i N_i f_i \,.$$

In both relations, contributions from shape anisotropies resulting from the particle's anisomery and differences between the mean optical (and magnetic) susceptibilities and those of the solvent have been neglected. This is generally justified for $\Delta\chi$ because of the negligibly small difference between external and internal magnetic fields in diamagnetic solutions, but shape birefringence can be important for larger macromolecules and virus particles. We are mainly interested in determining the f_i since they contain information about the structure of the particles. The N_i values are usually known from chemical analysis and $\Delta\alpha_i$ and $\Delta\chi_i$ values are available for various groups (Sect. 4.2); thus from CM one can deduce a relation between the f_i values. This relation simplifies when $\Delta\alpha$ is known from other experiments such as flow birefringence, electric birefringence or depolarised light scattering.

A measurement of the *linear magnetic dichroism* $\varrho = (A_\parallel - A_\perp)/A$ consists in determining $A_\parallel$, $A_\perp$ and A, the optical absorbances for light propagating perpendicular to H and polarised parallel, perpendicular to H and unpolarised, respectively. The term ϱ is related to the magnetic orientation function ϕ defined

in Sect. 4.3.1 and to f_i. For example, if the groups (i) have non-overlapping absorbance bands and (e.g. the base pairs of DNA) the corresponding optical transition moment lies in the plane normal to the rotational symmetry axis of the diamagnetic tensor, ϱ is simply given by $\varrho = -3f_i\phi/2$ [4.245]. Hence in this case the relative magnitudes of the f_i's can be determined for all absorbing groups spectrometrically accessible in the experiment. Relative f_i values can also be obtained for overlapping dichroic bands though data analysis is less straightforward. Knowledge of $\Delta\alpha$ results in a determination of ϕ from magnetic birefringence and then absolute values of f_i can be determined from dichroism. Therefore if the number of groups which contribute to the optical and diamagnetic anisotropies in a bioparticle are limited to say 3 or 4, a combination of magnetic dichroism and birefringence may yield information about orientational order (i.e. f_i) of these groups; f_i values can be calculated for structural models and compared with experiment.

Following these lines the structures of several nucleic acid- and/or protein-containing bioparticles in solution have been studied by magnetic orientation. Cotton-Mouton constants were measured [4.92] on dilute solutions of the *rod-like bacteriophages* Pf1 and fd, which both consist of a cylindrical protein shell enveloping 6.5 % and 12.9 % (w/w) DNA, respectively. The data were interpreted in terms of the diamagnetic anisotropies of the α helices and aromatic amino acids in the coat protein and of the DNA bases, as $\Delta\alpha$ of a single virus in solution was determined separately from the saturation birefringence in high magnetic fields of a fully oriented polyelectrolytic liquid crystal (Fig. 4.12). It turned out that the contribution of DNA to $\Delta\chi$ is weak and that both the axes of the α helices and the planes of the aromatic amino acids are oriented parallel to the phage major axis. By using magnetic birefringence a temperature-induced conformation change occurring around 10 °C was observed for Pf1 in solution for the first time. Independently, f_i values for DNA and aromatic amino acids were estimated from the magnetic linear dichroism of completely oriented virus solutions (Fig. 4.20). The results from both techniques agree.

A similar high field CM study was carried out on the buoy-shaped bacteriophages T4 and T7 which contain about 50 % DNA as well as on their empty protein shells (ghosts) [4.246a]. It was found that the diamagnetic anisotropy of the protein shell is negligibly small and that in T4 about $f_i = 35$ % of the DNA packed inside the protein shell (in an unknown fashion) is oriented parallel to the phage's head-tail axis. Diamagnetic anisotropy was discovered recently [4.246b] even in some so-called spherical viruses, suggesting that anisotropic packing of nucleic acids might be quite common in compact biological structures.

Dilute aqueous solutions of *chromatin* (the DNA protein complex occurring in the eucaryontic nuclei) and of chromatin fragments (so-called *nucleosomes*) at low ionic strengths ($\leq 10^{-2}$ M NaCl) both showed about 3 times smaller CM constant than free DNA. This reduction in anisotropy quantitatively agrees with current structural models of chromatin, in which the DNA loops around the globular protein core, thus forming bead-like nucleosomes linked by free DNA.

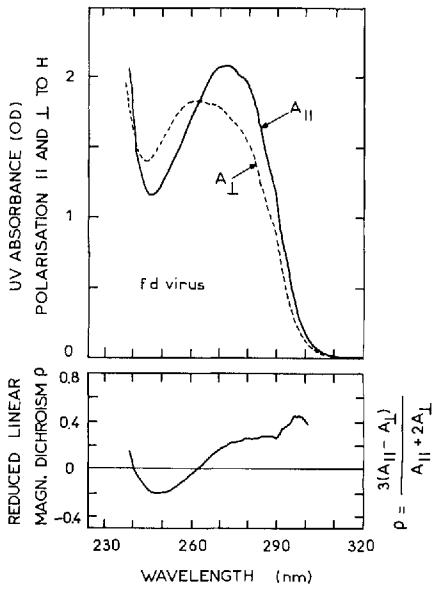

Fig. 4.20. The uv absorbance of magnetically oriented concentrated solutions of the cylindrical bacteriophage fd is strongly anisotropic (the magnetic linear dichroism saturates). The solution (at $c = 9.9$ mg/ml, 10^{-3} M Tris-HCl, pH 7.5) was oriented in a standard spectrometer cell (optical path 0.5 mm) by a vertical magnetic field of 12.2 T for 10 min, and appeared like the samples shown in Fig. 4.11b. The uv spectra were subsequently recorded for light polarised parallel and perpendicular to H; no disorientation could be observed within the first 30 min. Absorbance in the 240–260 nm and 270–300 nm regions mainly originates from the phage's DNA and aromatic amino acids, respectively. Both DNA bases and aromatic amino acids have in-plane, electronic transitional moments and the phage orients along H; therefore the negative (positive) dichroic bands observed for DNA (aromatic amino acids) indicate that the planes of DNA bases (aromatic amino aicds) are on the average more perpendicular (parallel) to the long axis of fd (Maret, unpublished result)

The results also suggest that the chain of beads is very flexible [4.6, 129]. It has been erroneously concluded from strong polarised and depolarised light-scattering signals that t-RNA, its shape being approximated by a prolate ellipsoid of revolution, aligns *along* a magnetic field [4.247]. A detailed analysis of the reported data [4.247] revealed that t-RNA orients *perpendicular* to H and that the dominant part of the aromatic base planes are preferentially perpendicular to the particles long axis [4.248]. This agrees with the observed negative birefringence and positive Cotton-Mouton constant of t-RNA. Probably the anisotropic light scattering originated from large anisometric aggregates.

Experimental Cotton-Mouton constants of dilute solutions of *fibrinogen*, an elongated protein involved in blood coagulation (Sect. 4.4), have been analysed in comparison with the rod-like bacteriophages fd and Pf1. From this it seems likely that fibrinogen contains about 30 % α helices oriented along the molecular long axis [4.249].

Murayama's microscope observation [4.250] clearly demonstrated that sickle cells, which are anomalously deformed *erythrocytes*, align with their long axis perpendicular to a field of only 0.35 T. *Costa Ribero* et al. [4.251] confirmed this recently and obtained a diamagnetic anisotropy of 2.7×10^{-18} erg/G^2 per sickle cell. They pointed out that this large anisotropy can be quantitatively accounted for by the paramagnetic anisotropy of the haeme group (Sect. 4.2) of the protein haemoglobin confined in the cell. Haemoglobin molecules in sickle cells are condensed into parallel fibres which are oriented along the cell's long

axes. Within the fibres the average orientation of the haeme planes is almost normal to the fibres; thus alignment of the cell axes normal to H corresponds to strong orientation of the haeme planes along H, as expected (Sect. 4.2). There seems to be no need to include contributions of the cell membrane to $\Delta\chi$.

Leitmannova et al. [4.252] reported that abnormally shaped erythrocytes occur at higher density in a sample after exposure (for typically 10 min) to a 1.0 T magnetic field. In addition, about 10 % of erythrocytes were damaged ("haemolysed") in 1 T. Since this amount increased more than linearly with H, one could expect full haemolysis to take place in fields above 8–10 T. However, others [4.253] have found that less than 1 % of erythrocytes, if any, are haemolysed after 10 min exposure of blood to 20 T.

Cotton-Mouton constants and partial saturation of the magnetic birefringence in fields above 6 T have been reported [4.254] for suspensions of a peptidoglycanteichoic acid complex, the major component of a *bacterial cell wall*. The dominant contribution to $\Delta\chi$ seems to come from the ordered cross-linked polysaccharide chains within the cell wall. A quantitative analysis of these data appears to be difficult because $\Delta\alpha$ is not known, the particles are much larger than optical wavelengths (Sect. 4.3.1) and presumably polydisperse; since they have a closed sac-like shape, contributions to the birefringence could also originate from magnetic deformation.

4.4 Polymerisation Reactions and Locking of Alignment in High Magnetic Fields

A long-range orientational order makes possible strong magnetic alignment even of weakly diamagnetically anisotropic molecules in modest fields. For various applications, it is of interest to stabilise the aligned phase (e.g. by freezing, crystallising, drying, polymerising, cross-linking or other ways of gel formation). *Sobajima* [4.91] was the first (1967) to produce strongly oriented films of partially crystallised α helices by *slowly drying* a lyotropic solution of poly-γ-benzyl-L-glutamate (PBLG) in 0.7 T. These and other magnetically oriented and dried films or fibres, including poly-γ-ethyl-glutamate, polynucleotides and rod-like viruses, have become useful for structural studies mainly by x-rays, but also by optical, NMR and other techniques [4.5, 91, 152, 153, 158, 159, 161, 167, 178, 183, 185, 255]. As an example, Fig. 4.21 shows the oriented x-ray pattern from the two polymers DDA-8 and DDA-9 (cf. Fig. 4.8) with nematogenic groups in the main chain. One sample (a) was slowly *cooled* from the nematic melt below the crystallisation temperature in a vertical 16 T field. Strongly oriented crystallites result. The other (b) was rapidly *quenched* and the magnetically oriented nematic structure was preserved at room temperature.

Finer and *Darke* [4.170] obtained an oriented gel of poly-L-lysine-hydrobromide by cooling a concentrated aqueous solution through the liquid-gel transition temperature in 1.45 T. *Avirom* [4.256] stabilised the magnetic

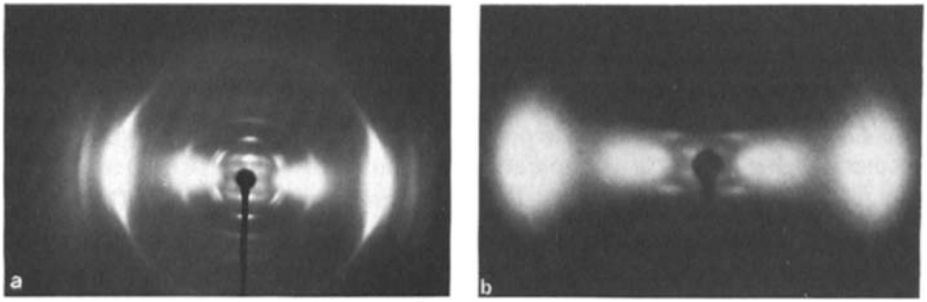

Fig. 4.21a, b. Oriented partially crystalline (**a**) or quenched nematic (**b**) phases can be produced when melts of polymers with liquid crystalline (nematogenic) groups in the main chain are slowly (**a**) or rapidly (**b**) cooled in a strong magnetic field from the nematic phase into the solid state. The x-ray patterns were taken from samples contained in 1 mm diameter capillaries with the x-ray beam normal to the magnetic field. (**a**) DDA-8 oriented by a vertical field of 16 T at 235 °C, cooling rate 1°/min to room temperature. (**b**) DDA-9 quenched in 12 T at 100°/min. The most outward equatorial reflection corresponds to a spacing of about 0.4 nm [4.183, 185]

orientation in PBLG by intermolecular chemical *cross-linking* with amide bonds between benzyl-alcohol groups. In 1973 *Liebert* and *Strzelecki* [4.257] introduced *polymerisation* under magnetic fields as a tool to produce oriented bulk polymers. A mixture of two types of nematic monomers (p-acryloyloxybenzylidene p-cyano-aniline and di-p-acryloyloxybenzylidene p-diamino-benzene) copolymerised in 0.8 T resulted in an oriented crystalline phase which was almost free of defects. *Perplies* et al. [4.8] polymerised a methacrylic Schiff base in strong magnetic fields (7 T) and obtained an oriented polymer matrix, but only from the nematic and not from the isotropic phase of monomers. These authors also showed, in agreement with *Clough* et al., *Cser* and *Lorkowski* and *Reuther* [4.258–260], that a magnetically oriented nematic monomer can yield a polymer with smectic ordering. *Torbet* et al. [4.249] investigated for the first time a *biological polymerisation* process in magnetic fields; they found a highly oriented filamentous fibrin network when polymerising – as during blood coagulation – the blood plasma protein fibrinogen in fields up to 20 T. From neutron-diffraction patterns of these oriented gels (Fig. 4.22) new features of the structure and packing of the fibrin protofibrils inside the fibrous network could be obtained; structural information about fibrinogen and fibrin can be expected from the study of such magnetically oriented samples.

In addition, *Perplies* et al. and *Torbet* et al. [4.8, 9] have shown that the application of a magnetic field is needed – at least in some cases – only during primary stages of polymerisation. As indicated in Fig. 4.23, the orientation persists to increase after switching off the field, once an oriented polymer matrix has started to form. From such measurements it seems possible to gain new insight into the complex microscopic processes involved in the formation of microfibrils and gels during polymerisation or polycondensation. At present, however, the influence of molecular orientation on the reaction kinetics is not

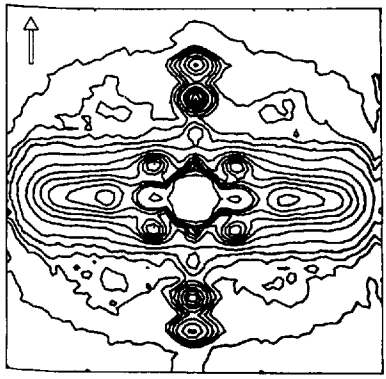

Fig. 4.22. Neutron diffraction pattern from fibrin gels ($c = 10$ mg/ml in H_2O buffer) oriented in a vertical magnetic field of 18 T. The 22.5 nm period meridional reflections presumably arise from a half staggered arrangement of monomers along the fibre axes and the 19 nm equatorial peak originates from the lateral protofibril packing [4.9]

well understood. For example, *Perplies* et al. [4.8] observed a 40 % *increase* in the polymerisation rate of bulk nematic monomers oriented by 7 T, whereas *Wojtczak* [4.261] found a strong *inhibition* of acetic aldehyde polymerisation in aqueous solution by fields of only 0.6 T. It was reported recently [4.262] that the gelation temperature of aqueous solutions of the polysaccharide agarose increases by 2 °C in 1 T. The significance of this observation seems unclear when compared with the very small shift of the nematic-isotropic transition temperature (Sect. 4.3.3a).

It is evident that magnetic fields can be used to bring molecules into a stable strongly oriented form well suited for structural analysis. The most important

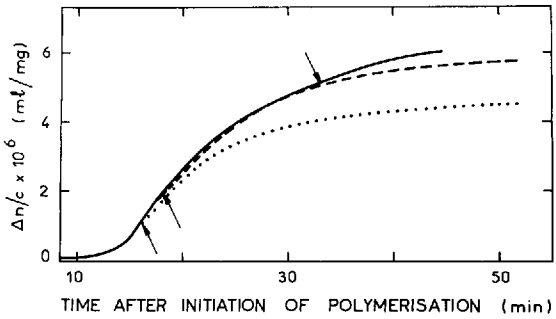

Fig. 4.23. Specific birefringence $\Delta n/c$ during polymerisation of fibrin in a strong magnetic field (11 T), initiated at $t = 0$ by adding the activating enzyme thrombin to a 5 mg/ml solution of fibrinogen. As polymerisation proceeds the growing fibrin fibres become sufficiently large and anisotropic to be strongly orientable prior to substantial network formation. Arrows indicate instances of switching off the magnetic field. (The lowest, middle, and upper arrow belong to ···, – – –, ——, respectively). In all three cases (···, – – –, ——) the orientation futher increases even in zero field, indicating that the orientation of fibres becomes fixed in the forming network and that the final reaction step is fibre growth. The maximum value of $(\Delta n/c)$ corresponds to nearly complete alignment of the polymer filaments, as seen independently by scanning electron microscopy and neutron diffraction [4.9, 249]

requirement for a successful application of this technique to produce alignment seems to be the existence of a highly ordered *liquid* (say liquid crystalline or fibrous) state prior to solidification. In contrast to usual mechanical orientation techniques, no elastic gel state with polymeric entanglements is needed and the orienting field can be applied steady state to small samples of any shape.

4.5 Separation of Macromolecules in Magnetic Field Gradients

In homogeneous magnetic fields, an orientational but no translational force acts on an *anisotropic* particle. In inhomogeneous fields, however, a translational force exists even for *isotropic* particles; it depends on the variation of H across the particle, i.e. grad(H^2), on the excess susceptibility of the particle as compared to the susceptibility of the surrounding medium and on its volume. In weakly diamagnetic media, ferromagnetic and paramagnetic particles are attracted into the high field region and diamagnetic particles are weakly repelled. These forces have been well described [4.263–4.266 and references therein] and various devices combining strong homogeneous magnetic fields with high gradients near ferromagnetic edges or wires have been developed and succesfully applied to separate ferro- or paramagnetic particles as small as a few microns in diameter. Promising applications range from filtration of low-grade iron ores and desulphurisation of coal to purification of waste water. This work has been reviewed by *Oberteuffer* and his colleagues [4.263, 267].

Separation is efficient when the magnetic force overcomes thermal agitation and gravitational forces. It builds up on a time scale controlled by the viscosity of the solvent. To separate diamagnetic particles or macromolecules of given size, shape and weight, the product $H \cdot \text{grad}H$ should be maximised. Near a ferromagnetic wire or edge in a strong external field $H_0 (> M_s)$ the field drop – excess over H_0 – approaches a limit, which is just the saturation magnetisation of the ferromagnetic material (M_s), and spatially extends over a distance comparable to the surface radius of curvature R, hence grad$H$ approximately equals M_s/R. Since R should not be smaller than the dimension of the particle or macromolecule to be separated, M_s/R is limited and higher separation efficiency can be obtained only by applying a stronger external field H_0, $H \cdot \text{grad}H$ approaching $H_0 \cdot M_s/R$. Following these lines, *Gill* et al. [4.265] reported in 1960 the diamagnetic susceptibility of polystyrene latex and red blood cells from visual observation of the drift velocity (of typically 1 μm/s) in inhomogeneous fields ($H \cdot \text{grad}H \simeq$ some $\text{T}^2\,\text{cm}^{-1}$). *Melville* et al. [4.31, 268] separated deoxygenated, paramagnetic red blood cells without damage from normal blood flowing at velocities around 1 cm/min throughout a randomly coiled steel wire within a magnetic field; the $H \cdot \text{grad}H$ value near the wire was estimated to be about $130\,\text{T}^2\,\text{cm}^{-1}$. *Owen* [4.32] used a similar experimental set-up and similar conditions to separate paramagnetic methaemoglobin erythrocytes from diamagnetic oxygenated erythrocytes or leucocytes. Magnetic migration of ery-

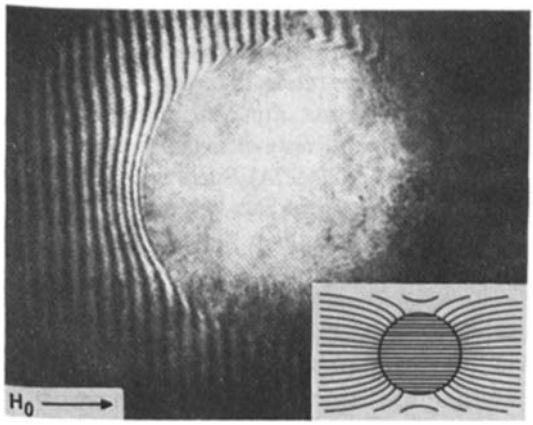

Fig. 4.24. Interferometric observation of the magnetosedimentation of the globular protein bovine γ-globulin in dilute aqueous solution. A cylindrical cell containing the solution and a coaxial steel cylinder (grey central region) is placed in one branch of a Jamin-type interferometer and is photographed end on. This optical set-up implies that at zero magnetic field, the uniform protein concentration (uniform refractive index) results in straight optical interference fringes (not shown); if a horizontal magnetic field H_0 of 1.2 T is applied perpendicular to the ferromagnetic cylinder, the field gradient near its surface as sketched in the insert creates a concentration gradient (refractive index gradient) which causes the interference fringes to bend [4.30]

throcytes was also noted by *Porath-Furedi* and *Yanai* [4.269]. By an optical interference technique *Simonsen* and *Gill* [4.30] were able to demonstrate a concentration gradient even of smaller proteins, the 169,000 molecular weight bovine gamma-globulin, in aqueous solution (containing a paramagnetic salt) building up within typically 10^2 min in $H \cdot \mathrm{grad} H \simeq 100\,\mathrm{T^2\,cm^{-1}}$ close to a ferromagnetic rod (Fig. 4.24). By this method it was possible to determine the diamagnetic susceptibility of macromolecules in solution even at substantial dilution.

Selective removal of small diamagnetic (bio)-particles from suspension can also be achieved in fairly low fields and gradients if a complex with ferromagnetic particles is formed. This was first demonstrated by *Bitton* and *Mitchell* [4.270] on bacteriophage T7 bound onto magnetic particles, using a steel wool filter and only 0.1 T. More recently so-called ferrofluids have become important in this field. They are suspensions of ultramicroscopic ($\lesssim 100$ nm) ferromagnetic particles coated by polyelectrolytes which prevent interparticle agglutination. Coating the ferromagnetic particles by polymers which were specifically substituted with certain enzymes enabled *Mosbach* and *Andersson* [4.271] to remove the latter magnetically, thus avoiding the usual centrifugation and column chromatography steps. Similarly, when coated by a special polymer carrying a specific cell-surface ligand, magnetic ferrofluids were used to separate whole neuroplastoma cells in $0.1\,\mathrm{T^2\,cm^{-1}}$ with better than 99 % efficiency under sterile conditions within only a few minutes [4.272]. Also drugs were con-

centrated magnetically at specific sites in organisms [4.273]. Obviously the chemical variety of coating polymers on ferromagnetic particles opens a wide field of applications for high gradient magnetic separation in biology and related fields.

Another way of enhancing the magnetic susceptibility of biological materials is to add strongly paramagnetic ions such as erbium [4.274]. Since Er^{3+} ions have a magnetic moment of 9.5 Bohr magnetons and bind to negatively charged surfaces, magnetic separation becomes more efficient.

4.6 Influence of Magnetic Fields on Living Cells

In this section we mention some newer findings demonstrating the interaction of magnetic fields (including weak fields) with more complex living systems. The microscopic processes involved are scarcely understood in many cases. We add some speculative remarks on how some biomagnetic effects could be related to the *magnetic properties* of the constituent molecules.

The work in "magnetobiology" (effects of external magnetic fields on biological matter) has been reviewed [4.34–36, 275–279]. The rapidly growing field of "*biomagnetism*" (weak magnetic fields created by living matter), which is beyond the scope of this article, has been reviewed by *Williamson* et al. and *Geselowitz* [4.280, 281].

4.6.1 Magnetic Field Detection by Animals

During the last decade strong evidence has been accumulated demonstrating that various animals ranging from simple amoebia and bacteria to sharks and homing pigeons are able to detect weak magnetic fields such as the earth's field (survey in [4.38–42]). Pigeons and bees seem to be sensitive to field variations some thousand times below the earth's field level. At least in some cases the animals are known to use this sense for orientation and navigation purposes. *Volvox* – an evolutionary very simple organism and a direct descendant of one of the earliest forms of life – can distinguish between magnetic fields of different intensities and directions [4.282]. This suggests that sensitivity to magnetic fields might be a rather general and important feature of living matter.

A first hint that ferromagnetic particles might be involved in a magnetic field "sensor" mechanism arose in *Blakemore* and colleagues' work on *bacteria* [Refs. 4.34, p. 354; 4.39, 43, 283]. They observed that some classes of bacteria migrate spontaneously towards geomagnetic north. This property seems to be essential for survival of the bacteria, since by swimming north along the earth's field lines, which are inclined towards the ground in the northern hemisphere, the bacteria always return to their optimal environment in the mud. These so-called magnetotactic bacteria synthesise almost cubic, ~ 50–100 nm sized, ferromagnetic monodomain magnetite particles. Each bacteria contains about 20 such

particles aligned in a chain so that the total magnetisation points along the bacterial major axis. This compass needle like device is just large enough to allow alignment in the earth's field against thermal agitation [4.284]. It turned out that there is no north-south ambiguity in this device: bacteria in the southern hemisphere do swim towards south because their chains are magnetised in the opposite direction [4.285]. Magnetite is synthesised in the bacteria with headwards or tailwards magnetisation at about equal probability, but only the species with correct magnetisation polarity seems able to survive in a given hemisphere, except near the equator. Other simpler animals responding to the earth's magnetic fields are snails [4.286] and salamanders [4.287]. Amongst insects, flies (*Drosophila*) [4.288], *sandhoppers* (*Tenebrio* and *Talitrius*) [4.289] and more intensely *bees* and *hornets* [4.44, 277, 290, 291] have been successfully studied. Bees exhibit a certain "Missweisung" (deviation from the correct orientation) of their dancing figures and construct their combs in certain directions, both being related to the earth's magnetic field. They eventually adjust their circadian rhythm to small diurnal variations of the earth's field. In their abdomen, ~ 100 nm particles of magnetite have been found [4.44] and the amplitude and direction of the overall magnetisation have been measured directly by a SQUID magnetometer.

Magnetite was also found recently in *dolphins* [4.292] and *rays* [4.293]. It would be premature, however, to conclude from this that the magnetic sensibility of animals can generally be explained in terms of ferromagnetic "compass needles". Beautiful training experiments by *Kalmijn* [Refs. 4.40, p. 347; 4.294] on *elasmobranch fish* (sharks, skates and rays) demonstrated their ability on the one hand to orient magnetically, and on the other hand to detect electric fields as small as 10 nV/cm by their organ ampullae of Lorenzini located in the skin; since electric fields of such weak strength are in fact induced in the fish by swimming through the earth's magnetic field, an electrodynamic compass system might exist as well. *Jungermann* et al. [4.295] discussed the labyrinth of the inner ear as a possible location for the induction loop.

Various *migrating birds* like robins [4.296], warblers [4.297], indigo buntings [4.298] and blackcaps [4.299] have a magnetic compass. *Wilschko* and *Wilschko* showed that robins do not use the polarity of the magnetic field to determine north, but only its inclination with respect to gravity; there is a maximum in sensitivity at magnetic fields comparable to the earth's magnetic field. An increasing number of studies has been published (surveys in [4.42, 300, 301a, b]) in the past years on the magnetic sense of *homing pigeons*, mainly initiated by work of *Keeton* [4.302] and *Walcott* and *Green* [4.303]. They showed that superimposing an artificial magnetic field on the earth's magnetic field by fixing small bar magnets or Helmholtz coils to the pigeons' head caused a substantial loss in their orientation capability. Pigeons integrate some information about the earth's field during transport from the loft to the release site [4.304] and possibly possess a "geomagnetic map" [4.301] in addition to the magnetic compass system. Monodomain elongated magnetic particles (~ 100 nm) have been

discovered [4.46] in tissues of pigeons too, apparently located between the pigeons' brain and skull [4.46, 305] and in the neck musculature [4.300].

Studies on humans have been controversial so far. *Baker* [4.306, 307] reported the ability of blindfolded humans to indicate the homeward direction when carried away from home; this ability apparently disappeared when the earth's magnetic field was strongly perturbed in the head region using Helmholtz coils mounted around the head. Attempts to reproduce this observation were not successful [4.308]. *Kirschvink* found magnetic remanence in human adrenal tissue [4.309].

Besides the "ferromagnetic" and "inductive" compass mechanisms [Refs. 4.34, p. 287; 4.310] other types of earth's magnetic field detectors in animals have been proposed. *Gunter* et al. [4.311] suggested that the animal detects a movement of large particles or organelles inside a cell due to the drag caused on them by the ionic currents if the cell is exposed to crossed internal electric and external magnetic fields. This electrophoretic process in a magnetic field leads to a (linear) increase of the particles' speed with H, and one might speculate that exposure of the animal to very strong magnetic fields would cause severe deviations. Other models of "magnetoreception" involving diamagnetic or paramagnetic properties of living material or optical pumping into magnetically split triplet states have recently been discussed and criticised by *Leask* [Ref. 4.40a, p. 318].

In birds the "induction" model does not seem to be appropriate mainly because of the finding that even a magnetic field produced by coils which *moved* with the bird (and thereby produced no induction) did perturb the bird. A mechanism involving the magnetic particles seems to be very attractive in the sense that it disagrees with neither experimental nor theoretical findings [4.312–315]. The physics of small monodomain or superparamagnetic particles in a magnetic field is well understood [4.314], however, little is known about the coupling mechanism of these particles to the nervous system. *Presti* and *Pettigrew* [4.300] suggested that some sensory fibres in the muscles particularly sensitive to stretch might be involved. *Kirschvink* and *Gould* [4.314] proposed four types (1–4) of "magnetoreceptors". The first (1) implies freely rotatable monodomain magnetite particles embedded in a membrane. The particle is coated with some electrically insulating material except for the regions at the magnetic poles. Since magnetite is a good conductor an orientation of the particle with the magnetic field normal to the membrane would open a conducting channel across the membrane. In (2) a superparamagnetic magnetic particle is locked into the membrane. In this case the magnetisation aligns without rotation of the particle in an external field; the transmembrane conduction change is performed by orientation of nearby membrane proteins ("satellites") which have ion pores and carry small magnetic rods. In (3) the torque in a magnetic field on a chain of monodomain particles would be detected by some mechanoreceptor, for example a hair cell. Detector (4) involves an array of regularly spaced superparamagnetic particles embedded in an elastic medium. Magnetic interparticle interaction stresses the elastic medium, the stress

depending on the direction of an external field. Other mechanisms or combinations of (1–4) could be imagined. Obviously a direct, perhaps electron-microscopic observation of such an organelle would best elucidate the actual situation. Another approach is to expose the animal to a strong external field with and without field gradients and then test its navigational performance.

Such experiments on pigeons were actually performed in our laboratory [4.316]. Submitted to steady fields of up to 10 T for 2 min, the pigeons did not show any sign of harm during exposure. However, their average vanishing direction, when released some 50 km from the loft, deviated (by some 40°–50° to the left) from the homing direction taken by the unexposed control group of pigeons [4.316]. Vanishing bearings from experimental and control pigeons both showed the normal amount of scattering around the vanishing direction. These results indicate that some modifications were caused by the strong field and lasted for at least several days. If effects of field gradients can be neglected, the data would not be consistent with detector mechanisms (1) and (2) because the free rotatability of the magnetite particles should not be permanently affected by a strong field. Torque and stress in (3) and (4) might have gone beyond a certain yield limit during exposure and permanent damage occurred; this does not seem very probable because of the observed normal behaviour of the pigeons during exposure and the lack of increased scattering in their vanishing bearing. In the framework of (1–4) we would thus be left with the possibility that some change in the direction of magnetisation in the torque detector (3) occurred. Further studies of this kind should certainly include strongly inhomogeneous fields and perhaps ac fields, the latter to search for the possibility of demagnetisation.

4.6.2 Growth in Magnetic Fields

Audus [4.47, 317] was the first to observe an influence of the magnetic field on the direction of growth in plants (magnetotropism). Compensating for gravitropism (by slow rotation of the experimental set-up around the horizontal direction of initial growth) he found that both cress *roots* and oat *shoots*, initially aligned along the pole shoes perpendicular to a 0.4 T field, tended to grow into regions of weaker magnetic fields by bending. One might think that the negative magnetotropism could be due to the overall force acting on the diamagnetic body of the root or shoot in the magnetic field gradient of about 0.6 T/cm (Sect. 4.5). However, when the plants grew along the planar surface of an agar gel, which had been oriented parallel to the magnetic field but normal to the field gradient and was sufficiently rigid to withstand this force, magnetotropism could still be observed. Hence this latter force could not be the physical origin of Audus' observation. He also demonstrated that the mechanisms involved in magnetotropism cannot be related to gravitropism, since, in contrast to the case of graviperception, no magnetically induced intracellular displacement of statoliths was observed nor did roots and shoots show a different sign of the *magneto*response.

Therefore one might speculate that magnetotropism is caused by a magnetic field dependence of the local growth rate. The negative magnetotropism mentioned above could originate from an accelerated cell elongation or an enhanced cell division rate in the region of stronger magnetic field strength; in addition, both elongation and division could depend on the direction of the applied magnetic field.

Hence, it seems very important for the understanding of Audus' experiment to search for magnetotropism in less complex, monocellular or non-dividing systems. On these lines *Schwarzbacher* and *Audus* have investigated [4.318] magnetotropism of the monocellular spore *phycomyces* in strong field gradients. Recently magnetotropism was observed even in homogeneous magnetic fields. As demonstrated by Fig. 4.25, *Sperber* et al. [4.49] found that the elongational growth of monocellular pollen tubes of lily is almost completely oriented parallel to a homogeneous strong magnetic field. The orientational distribution function is bimodal and symmetric, i.e. magnetic north and south are equivalent. In addition, in inhomogeneous strong fields, a preferential growth of the tubes into regions of lower magnetic fields was found (Fig. 4.26). These observations on non-dividing cells indicate that magnetotropism is not necessarily related to magnetic orientation of ordered macromolecular arrays as occurring during cell

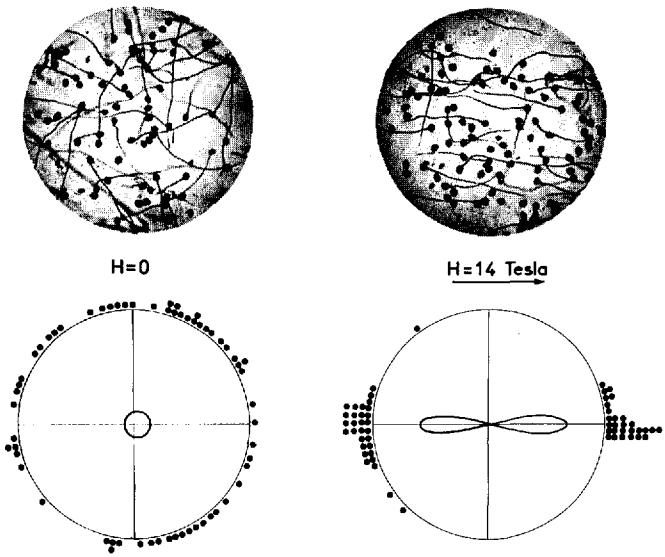

Fig. 4.25. Pollen tubes of lily show a strongly oriented elongational growth in *homogeneous* high magnetic fields (magnetotropism). The photographed tubes and grains (diameter typically some 100 μm) have grown for 3 h at 30 °C on the surface of agar gel inside a horizontal Bitter magnet without magnetic field (*left*) and in 14.0 T horizontal field (*right*). A polar representation of the orientational distribution function (best fit through the black data points) is given underneath for each sample. The radial distance from the origin is proportional to the number of tubes found with a tip direction within a 10° interval around the azimuthal angle θ [4.49]

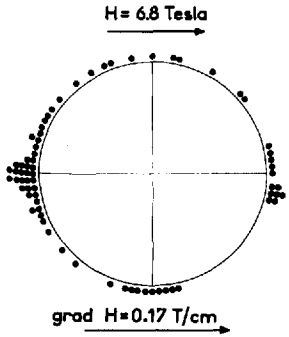

Fig. 4.26. Magnetotropism of pollen tubes of lily in *inhomogeneous* fields. Growth conditions were similar to those indicated in Fig. 4.25. The sample was placed on the axis of a horizontal solenoid but off centre, i.e. in the region of the axial field gradient ($H = 9.7$ T, grad $H = 140$ T/m). Superimposed on the bimodal orientation (of Fig. 4.25) is a unimodal component indicating the tendency of growth into regions of smaller magnetic fields [4.49]

division. Perhaps the mechanisms involved are much simpler than expected previously. A full field strength dependence of the magnetotropism of pollen tubes has not been evaluated yet, but this phenomenon is a typical high field effect: tubes grown for 9 h in only 3 T showed hardly any orientation.

We add some speculative remarks on magnetic field induced modification of growth which could be involved in magnetotropism.

First the *elongational growth* of single cells could possibly be enhanced because of accelerated *metabolism* in the magnetic field: some indirect evidence for modified ion transport across membranes has been discussed by *Aceto* et al. [4.278] and *Amer* and *Tobias* [4.319]. More recent findings that action potential [4.320] and conduction velocity [4.321] of frog sciatic nerve are enhanced in fields around 1 T might also be interpreted in terms of structural changes in membranes. This latter field has been critically reviewed by *Schwartz* [4.321, 322]. Since such effects should depend on the direction of the magnetic field with respect to the membrane, they possibly also could imply some anisotropic elongational growth. On the other hand, the membrane material built in the cell wall during elongational growth is supplied by intracellular vesicles which undergo fusion with the membrane in the regions of growth, which is the tip region in the case of pollen tubes. When deformed during the *fusion process* these large ($\sim$several micron) vesicles presumably have a sufficiently high diamagnetic anisotropy to imply different probabilities for fusion into parts of the cell wall parallel and perpendicular to the magnetic field; as a result the elongational growth should become anisotropic.

There are some indications from biological experiments that *cell division* can be influenced by magnetic fields. *Mericle* et al. [Ref. 4.34, Vol. 1, p. 183] reported evidence for enhanced cell division rate in particular when a magnetic field was applied to the zone of cell multiplication (meristem) of barley roots; furthermore effects of steady magnetic fields have been observed on mitosis [4.323] and meiosis [4.324], embryonic development [4.325–327], growth of yeast (summarised in [4.328]) and on the fertility of small fish during several life cycles [4.329]. Keeping in mind the anisotropic diamagnetic properties of various biological macromolecules, and the existence of highly ordered liquid crystalline

states *in vivo* particularly during cell division, one might speculate that magnetic fields, imposing orientations for instance on metaphase chromosomes, spindles, membrane lamellae and the cell wall, favour certain polarities of the dividing cell. Obviously, microscopic observations of cell multiplication in a strong magnetic field could help to explain some magnetobiological effects.

Finally we draw attention to the prediction made by several authors [4.330–333] that the stream of electrically conducting blood in large arteries can be reduced dramatically by a strong transverse magnetic field. It follows from classical magnetohydrodynamics that, for example, in a tube of 1 cm diameter and in 20 T the natural mean streaming speed should be slowed down by a factor of two. It should be easy to verify this effect directly by experiment, which promises various applications.

Recently *Gremmel* et al. [4.334] discovered that magnetic fields as commonly used in NMR tomography can cause sizeable temperature changes ($\Delta T \approx 5\,^{\circ}\mathrm{C}$) in those parts of the human body which are exposed to the magnetic field. Magnetic-field-induced temperature changes ($\Delta T \approx 2.5\,^{\circ}\mathrm{C}$) were also observed by *Sperber* et al. [4.335] in mice exposed to strong magnetic fields. Interestingly, in inhomogeneous fields the sign of the temperature change could be inverted if the gradient of the field relative to the animals' polarity was reversed.

Acknowledgements. The experimental work cited here was performed in close cooperation with many colleagues. They include A. Mayer, R. Oldenbourg, R. Ranvaud, M. v. Schickfus, E. Sénéchal, D. Sperber, M. Stamm and J. Torbet from our own laboratory. A. Domard, Y. Filippini, G. Fillion, J. M. Freyssinet, G. Hudry-Clergeon, J. J. Lawrence, B. Malraison, C. Meyer, H. Milas, R. Oberthür, Y. Poggi, F. Porte-Cuault, G. Porte, M. Rinaudo, K. Simpson and F. Volino are from various research institutions at Grenoble. Furthermore A. Blumstein, R. Blumstein (University of Lowell, Mass.), E. Fischer, M. Happ and H. Ringsdorf (University of Mainz), J. Kiepenheuer and K. Schmidt-Koenig (University of Tübingen), D. Marvin and his colleagues (European Molecular Biology Laboratory, Heidelberg), M. Showe (Biozentrum, Basel), G. Weill (CNRS, Strassbourg) and M. H. Weisenseel (University of Karlsruhe) were involved in parts of this work. Their contributions are gratefully acknowledged.

We should also like to thank our French colleagues from the Service National des Champs Intenses and M. Bichler, H. Dresler and A. Köhler for technical help.

Fruitful discussions with G. Eilenberger (KFA, Jülich), P. G. de Gennes (College de France, Paris), R. Klein (University of Konstanz), M. Papoular (CNRS, Grenoble), P. Pincus and P. Chaikin (University of California, LA) are acknowledged as well.

We are grateful to A. A. Bothner-By (Carnegie Mellon University Pittsburgh), E. Oldfield (University of Illinois, Urbana), H. Rüterjans (University of Münster), and K. Wüthrich (ETH, Zürich) for very instructive correspondence and communication of some work including photographs prior to publication. Thanks are due also to Mrs. Landsberg and Mrs. Rössler for carefully typing the final manuscript.

References

4.1 H.Kelker, R.Hatz, C.Schumann: *Handbook of Liquid Crystals*, (Verlag Chemie, Weinheim 1980)

4.2 G.Maret, M.v.Schickfus, A.Mayer, K.Dransfeld: Phys. Rev. Lett. **35**, 397 (1975)

4.3 G.Maret, J.Torbet, E.Sénéchal, A.Domard, M.Rinaudo, H.Milas: *Nonlinear Behaviour of Molecules, Atoms and Ions in Electric, Magnetic and Electromagnetic Fields*, ed. by L.Neel (Elsevier, Amsterdam 1979) p. 477
4.4 E.Sénéchal, G.Maret, K.Dransfeld: Int. J. Biol. Macromol. **2**, 256 (1980)
4.5 J.Torbet, G.Maret: J. Mol. Biol. **134**, 843 (1979)
4.6 G.Maret, K.Dransfeld: Physica **86–88B**, 1077 (1977)
4.7 N.Chalazonitis, R.Chagneux, A.Arvanitaki: C. R. Acad. Sci. **271**, 130 (1970)
4.8 E.Perplies, H.Ringsdorf, J.H.Wendorff: Polym. Lett. Ed. **13**, 243 (1975)
4.9 J.Torbet, J.M.Freyssinet, G.Hudry-Clergeon: Nature **289**, 91 (1981)
4.10 M.E.Michel-Beyerle, H.Scheer, H.Seidlitz, D.Tempus, R.Haberkorn: FEBS Lett. **100**, 9 (1979)
4.11 H.Rademaker, A.J.Hoff, L.N.M.Duysens: Biochim. Biophys. Acta **546**, 248 (1979)
4.12 A.J.Hoff, H.Rademaker, R. van Grondelle, L.N.M.Duysens: Biochim. Biophys. Acta **460**, 547 (1977)
4.13 M.C.Thurnauer, J.R.Norris: Biochim. Biophys. Res. Comm. **73**, 501 (1976)
4.14 J.Kalinowski, J.Godlewski: Chem. Phys. Lett. **36**, 345 (1975)
4.15 P.W.Atkins, G.T.Evans: Mol. Phys. **29**, 921 (1975)
4.16 P.W.Atkins: Chem. Phys. Lett. **18**, 355 (1973)
4.17 A.Gupta, G.S.Hammond: J. Chem. Phys. **57**, 1789 (1972)
4.18 L.R.Faulkner, A.J.Bard: J. Am. Chem. Soc. **91**, 6495 (1969)
4.19 H.Krath, H.Alms, J.M.D.Coey: J. Mater. Sci. **11**, 2283 (1976)
4.20 P.W.Selwood: Adv. Catal. **27**, 23 (1978)
4.21 N.Hata, Y.Yamanda: Chem. Lett. Jpn. 989 (Aug. 1980)
4.22 M.Sonneveld, L.N.M.Duysens, A.Moerdijk: Biochim. Biophys. Acta **636**, 39 (1981)
4.23 H.Hayashi, Y.Sakaguchi, S.Nagakura: Chem. Lett. 1149 (Sept. 1980)
4.24 K.Piotrowska, D.Edwards, A.Mitch, R.Dougherty: Naturwissenschaften **67**, 442 (1980)
4.25 P.W.Atkins: Recherche **10**, 118 (1979)
4.26 P.W.Atkins: *Physical Chemistry* (Oxford Univ. Press, Oxford 1978)
4.27 N.J.Turro, B.Kraeutler: Acc. Chem. Res. **13**, 369 (1980)
4.28 L.N.Mulay, I.L.Mulay: Anal. Chem. **52**, 199R (1980)
4.29 R.Stösser: Z. Chemie **17**, 201 (1977)
4.30 W.J.Simonsen, S.J.Gill: Rev. Sci. Instrum. **45**, 1425 (1974)
4.31 D.Melville, F.Paul, S.Roath: Nature **255**, 706 (1975)
4.32 C.S.Owen: Biophys. J. **22**, 171 (1978)
4.33 W.Haberditzl: Nature **213**, 72 (1967)
4.34 M.F.Barnothy (ed.): *Biological Effects of Magnetic Fields*, Vols. I, II (Plenum Press, New York, Vol. I 1964, and Vol. II 1969)
4.35 M.F.Barnothy, J.M.Barnothy: "Magnetobiology", in *Environmental Physiology* ed. by N.Balfour Slonim (Moshby, St. Louis 1974) p. 313
4.36 T.S.Tenforde (ed.): *Magnetic Field Effects on Biological Systems* (Plenum, New York 1979)
4.37 A.S.Presman: *Electromagnetic Fields and Life* (Plenum, New York 1970)
4.38 I.L.Gould: Am. Sci. **68**, 256 (1980)
4.39 R.B.Blakemore, R.B.Frankel: Sci. Am. **245**, 42 (Dec. 1981)
4.40 K.Schmidt-Koenig, W.T.Keeton (eds.): *Animal Migration, Navigation and Homing* (Springer, Berlin, Heidelberg, New York 1978)
F.Papi, H.G.Wallraff (eds.): Avian Navigation (Springer, Berlin, Heidelberg, New York 1982)
4.41 A.J.Kalmijn: IEEE Trans. Mag. **17**, 1113 (1981)
4.42 W.F.Keeton: Sci. Am. **231**, 96 (Dec. 1974)
4.43 R.B.Frankel, R.P.Blakemore, R.S.Wolfe: Science **203**, 1355 (1979); see also: Phys. Today **22** (Nov. 1979)
4.44 J.L.Gould, J.L.Kirschvink, K.S.Deffeyes: Science **201**, 1026 (1978)
4.45 J.L.Kirschvink, H.A.Lowenstam: Earth Planet. Sci. Lett. **20**, 193 (1978)
4.46 C.Walcott, J.L.Gould, J.L.Kirschvink: Science **205**, 1027 (1979)
4.47 L.J.Audus, J.C.Wish: In [Ref. 4.34, Vol. I, p. 170]

4.48 D.Sperber: Unpublished
4.49 D.Sperber, G.Maret, M.H.Weisenseel, K.Dransfeld: Naturwissenschaften **68**, 40 (1981)
4.50 R.A.Dwek: *NMR in Biochemistry* (Oxford Univ. Press, Oxford 1973)
4.51 G.Levy (ed.): *Topics in Carbon- 1 3 NMR Spectroscopy*, Vol. I (Wiley Interscience, New York 1974)
4.52 K.Wüthrich: *NMR in Biological Research: Peptides and Proteins* (North-Holland, Amsterdam 1976)
4.53 B.Pullmann (ed.): *Proceedings of the 3 3th Jerusalem Symposium on NMR*-Spectroscopy in Molecular Biology (Reidel, Dordrecht 1980)
4.54 K.Wüthrich, G.Wagner: Trends in Biochem. Sci. **3**, 227 (1978)
4.55 G.B.Lubkin: Phys. Today **32**, No. 11 (Nov. 1979) p. 17
4.56 A.A.Bothner-By, J.Dadok, submitted
4.57 E.Oldfield, T.M.Rothgeb: J. Am. Soc. **102**, 3635 (1980)
4.58 E.Oldfield: Private communication
4.59 F.Keilmann: J. Collect. Phenomena **3**, 169 (1981) and references therein
4.60 P.W.Selwood: *Magnetochemistry*, 2nd ed. (Interscience Publ. New York 1965)
4.61 W.Haberditzl: *Magnetochemie* (Akademie, Berlin 1968)
4.62 A.A.Bothner-By, J.A.Pople: Ann. Rev. Phys. Chem. **16**, 43 (1965)
4.63 M.R.Battagha, G.L.D.Ritchie: J. Chem. Soc. Faraday Trans. 2, **73**, 209 (1977)
4.64 K.Lonsdale: Proc. R. Soc. **171A**, 541 (1939)
4.65 K.Lonsdale, K.S.Krishnan: Proc. R. Soc. **156A**, 597 (1936)
4.66 R.Ditchfield: "Magnetic Suspectibility of Diamagnetic Molecules", in *MTP Int. Rev. Sci., Molecular Structure and Properties, Physical Chemistry*, Ser. 1, Vol. 2, ed. by A.D.Buckingham, Allen (Butterworth, London 1972)
4.67 J.W.Beams: Rev. Mod. Phys. **4**, 133 (1932)
4.68 A.D.Buckingham, J.A.Polple: Proc. Phys. Soc. **69**, 1133 (1956)
4.69 G.H.Meeten: J. Chim. Physique **7–8**, 1175 (1972)
4.70 L.Pauling: J. Chem. Phys. **4**, 673 (1936)
4.71 F.London: J. Chem. Phys. **5**, 837 (1937)
4.72 S.Yamaguchi; S.Okuda, N.Nakagawa: Chem. Pharm. Bull. **11**, 1465 (1963)
4.73 W.Zeil, H.Burchert: Z. Physik. Chem. Ser. 2, **38**, 47 (1963)
4.74 P.T.Marasimham, M.T.Rogers: J. Phys. Chem. **63**, 1388 (1959)
4.75 J.Guy, J.Tillieu: J. Chem. Phys. **24**, 1117 (1956)
4.76 T.Schaefer, Y.Yonemoto: Can. J. Chem. **42**, 2318 (1964)
4.77 A.Veillard, B.Pullman, G.Berthier: C. R. Acad. Sci. **252**, 2321 (1961)
4.78 G.Fillion, G.Maret: Unpublished
4.79 D.L.Worcester: Proc. Natl. Acad. Sci. (USA) **75**, 5475 (1978)
4.80 L.Pauling: Proc. Natl. Acad. Sci. (USA) **76**, 2293 (1979)
4.81 N.S.Murthy, I.R.Knox, E.T.Samulski: J. Chem. Phys. **65**, 4835 (1976)
4.82 K.Tohyama, N.Miyata: J. Phys. Soc. Jpn. **34**, 1699 (1973)
4.83 M.Kotani: Adv. Quant. Chem. **4**, 227 (1968)
4.84 N.Nakano, J.Otsuka, A.Tasaki: Biochem. Biophys. Acta **278**, 355 (1972)
4.85 P.G. de Gennes: *The Physics of Liquid Crystals* (Clarendon, Oxford 1974)
4.86 E.Cotton-Feytis, M.E.Faure-Frenniet: C. R. Acad. Sci. **214**, 996 (1942)
4.87 W.Arnold, R.Steele, H.Müller: Proc. Natl. Acad. Sci. **44**, 1 (1958)
4.88 N.E.Geacintov, F.V.Nostrand, M.Pope, J.B.Tinkel: Biochem. Biophys. Acta **226**, 486 (1971)
4.89 N.E.Geacintov, F.V.Nostrand, J.F.Becker, J.B.Tinkel: Biochem. Biophys. Acta **267**, 65 (1972)
4.90 F.T.Hong, D.Mauzerall, A.Mauro: Proc. Natl. Acad. Sci. **68**, 1283 (1971)
4.91 S.Sobajima: J. Phys. Soc. Jpn. **23**, 1070 (1967)
4.92 J.Torbet, G.Maret: Biopolymers **20**, 2657 (1981)
4.93 G.Weill: In *Molecular Electrooptics*, ed. by S.Krause (Plenum, New York 1981) p. 473
4.94 G.Maret, G.Weill: Biopolymers **22**, 2727 (1983)
4.95 M.P.Langevin: C. R. Acad. Sci. Paris **151**, 475 (1910)

4.96 A.Peterlin, H.A.Stuart: Z. Physik **112**, 1 and 129 (1939); and in *Optik* (Springer, Berlin, Heidelberg, New York 1933)
4.97 M.Born: Ann. Phys. **55**, 177 (1918)
4.98 W.Schütz: "Magnetooptik", in *Handbuch der Experimentalphysik*, Vol. 16, ed. by Wien-Harms (Akadem. Verlagsges., Leipzig 1936)
4.99 C.T.O'Konski, K.Yoshioka, W.H.Orttung: J. Phys. Chem. **63**, 1558 (1959)
4.100 M.J.Shah: J. Phys. Chem. **67**, 2215 (1963)
4.101 H.Geschka: Ph. D. Thesis, University of Ulm, FRG (1980)
4.102 K.Nagai, T.Ishikawa: J. Chem. Phys. **43**, 4508 (1965)
4.103 J.P.Flory: *Statistical Mechanics of Chain Molecules* (Wiley, New York 1969)
4.104 H.A.Stuart, A.Peterlin: J.Polym. Sci. **5**, 551 (1950)
4.105 L.D.Landau, E.M.Lifschitz: *Statistische Physik* (Akademie, Berlin 1970)
4.106 R.W.Wilson: Biopolymers **17**, 1811 (1978)
4.107 M.Stamm: Ph.D.Thesis, University of Mainz (1979)
4.108 E.W.Fischer, G.R.Strobel, M.Dettenmaier, M.Stamm, N.Staidle: Faraday Discuss. R. Soc. Chem. **68**, 26 (1979)
4.109 J.V.Champion, R.A.Desson, G.H.Meeton: Polymer **15**, 301 (1974)
4.110 M.Stamm, E.W.Fischer, G.Maret: Unpublished
4.111 A.E.Tonelli, Y.Abe, P.J.Flory: Macromolecules **3**, 294, 303 (1970)
4.112 A.Blumstein, G.Maret, S.Vilasagar: Macromolecules **14**, 1543 (1981)
4.113 G.Maret, A.Domard, M.Rinaudo: Biopolymers **18**, 101 (1979)
4.114 G.Weill, G.Maret: Polymer **23**, 1990 (1982)
G.Weill, G.Maret, T.Odijk: Polym. Comm. **25**, 147 (1984)
4.115 R.B.Meyer: Appl. Phys. Lett. **12**, 281 (1968)
4.116 P.J.Batchelor, J.V.Champion, G.H.Meeton: J. Chem. Soc., Faraday Trans. 2, **76**, 1610 (1980)
4.117 P.C.Nägele, L.Beck: Macromolecules **10**, 213 (1977)
4.118 A.A.Jones: J. Polym. Sci. Polym. Phys. Ed. **15**, 863 (1977)
4.119 G.H.Meeton: Polym. Lett. Ed. **15**, 187 (1974)
4.120 G.Maret, M. v. Schickfus, J.H.Wendorff: Coll. Int. CNRS, *Physique Sous Champs Magnétiques Intenses* **242**, 71, CNRS, Paris (1975)
4.121 V.N.Tsvetkov, G.I.Kudryavtsev, E.I.Ryumtsev, V.Nicolaev, V.D.Kalmykova, A.V. Volokhina: Dokl. Acad. Nauk. SSSR **224**, 398 (1975)
4.122 T.Odijk: Polymer **19**, 989 (1978)
4.123 P.Pfeuty: J. Phys. (Paris) **39**, C2-149 (1978)
4.124 J.Skolnick, M.Fixman: Macromolecules **10**, 944 (1977)
4.125 R.E.Harrington: Biopolymers **17**, 919 (1978)
4.126 K.L.Cairney, R.E.Harrington: Biopolymers **21**, 923 (1982)
4.127 P.J.Hagerman: Biopolymers **20**, 1503 (1981)
4.128 V.Rizzo, J.Schellman: Biopolymers **20**, 2143 (1981)
4.129 G.Maret: Ph.D. Thesis, University of Konstanz, FRG (1976)
4.130 B.Vollmert: *Polymer Chemistry* (Springer, Berlin, Heidelberg, New York 1973) p. 478
4.131 S.Sokerov, G.Weill: Biophys. Chem. **10**, 161 (1979)
4.132 J.E.Godfrey, H.Eisenberg: Biophys. Chem. **5**, 301 (1976)
4.133 R.Williams, R.Crandall: Phys. Lett. **A48**, 225 (1974)
4.134 A.Klug, R.E.Franklin, S.P.F.Humphreys-Owen: Biochim. Biophys. Acta **32**, 203 (1959)
4.135 J.D.Bernal, J.Fankuchen: J. Gen. Physiol. **25**, 111 (1941)
4.136 G.J.Oster: J. Gen. Physiol. **33**, 445 (1950)
4.137 R.J.Goldacre: Nature **174**, 732 (1954)
4.138 J.H.M.Willison: J.Ultrastruct. Res. **54**, 176 (1976)
4.139 For example: C.Robinson, J.C.Ward, R.B.Beevers: Discuss. Faraday Soc. **25**, 29 (1958)
4.140 L.Onsager: Ann. N. Y. Acad. Sci. **57**, 627 (1949)
4.141 A.Yu.Grossberg, A.R.Khokhlov: Adv. Polym. Sci. **41**, 53 (1981)
4.142 P.J.Flory, G.Ronca: Mol. Cryst. Liq. Cryst. **54**, 289 and 311 (1979)
4.143 M.Nierlich, C.E.Williams, F.Boné, J.P.Cotton, M.Daoud, B.Farnoux, G.Jannink, C.Picot, M.Moan, C.Wolff, M.Rinaudo, P.G. de Gennes: J. Physique **40**, 701 (1979)

4.144 T.Odijk: Macromolecules **12**, 688 (1979)
4.145 J.Mahanty, B.W.Ninham: *Dispersion Forces in Colloid Science*, ed. by R.H.Ottewill, R.L.Rowell (Academic, New York 1976)
4.146 V.A.Parsegian: Ann. Rev. Biophys. Bioeng. **2**, 221 (1973)
4.147 F.Oosawa: *Polyelectrolytes* (Marcel Decker, New York 1971)
4.148 G.Maret, J.Torbet: Unpublished
4.149 R.Oldenbourg: Ph.D. Thesis, University of Konstanz (1981)
4.150 R.Oldenbourg, G.Maret, K.Dransfeld: Proceed. 27th Int. Symp. Macromolec. (IUPAC) Strasbourg (1981)
4.151 L.Lapointe, D.A.Marvin: Mol. Cryst. Liq. Cryst. **19**, 269 (1973)
4.152 E.Jizuka, J. Tsi Yang: In *Liquid Crystals and Ordered Fluids*, Vol. 3, ed. by J.F.Johnson, R.S.Porter, (Plenum New York 1978) p. 197
4.153 E.Jizuka: Polym. J. **10**, 235 (1978)
4.154 E.Jizuka: Polym. J. **10**, 293 (1978)
4.155 E.Jizuka, Y.Kondo: Mol. Cryst. Liq. Cryst. **51**, 285 (1979)
4.156 G.Maret, M.Milas, M.Rinaudo: Polym. Bull. **4**, 291 (1981)
4.157 P.Pincus: J. Appl. Phys. **41**, 947 (1970)
4.158 E.T.Samulski, A.V.Tobolsky: Macromolecules **6**, 555 (1968)
4.159 Y.Go, S.Ejiri, E.Fukada: Biochim. Biophys. Acta **175**, 454 (1969)
4.160 E.T.Samulski, H.J.C.Berendsen: J. Chem. Phys. **56**, 3920 (1971)
4.161 E.T.Samulski, A.V.Tobolsky: Biopolymers **10**, 1013 (1971)
4.162 E.Jizuka: J. Phys. Soc. Jpn. **31**, 1205 (1971)
4.163 E.Jizuka: Polym. J. **4**, 401 (1973)
4.164 N.Miyata, K.Tohyama, Y.Go: J. Phys. Soc. Jpn. **33**, 1180 (1972)
4.165 E.Jizuka: Polym. J. **5**, 62 (1973)
4.166 E.T.Samulski: J.Physique Suppl. **40**, C3-471 (1979)
4.167 E.Jizuka: Mol. Cryst. Liq. Cryst. **27**, 161 (1973)
4.168 C.Guha-Shridhar, W.A.Hines, E.T.Samulski: J. Physique Suppl. **36**, C1-269 (1975)
4.169 J.R.Fernandes, D.B.DuPré: Mol. Cryst. Liq. Cryst. Lett. **72**, 67 (1981), and references therein
4.170 E.G.Finer, A.Darke: J. Chem. Soc. Faraday Trans., Sect. 1 **71**, 984 (1975)
4.171 A.Blumstein (ed.): *Liquid Crystalline Order in Polymers* (Academic, New York 1978)
4.172 A.Blumstein (ed.): *Mesomorphic Order in Polymers and Polymerization in Liquid Crystalline Media* (Am. Chem. Soc. Symp. Ser. 74, Washington 1978)
4.173 A.Ciferri, W.R.Krigbaum, R.B.Meyer (eds.): *Polymer Liquid Crystals* (Academic, New York 1982)
4.174 M.Happ, H.Ringsdorf, G.Maret: Unpublished
4.175 W.Pechold, S.Blasenbrey: Kolloid Z. Z. Polym. **241**, 955 (1970)
4.176 V.Tsvetkov, E.Frisman: Acta Phys. Chim. URSS **19**, 7 (1944)
4.177 J.V.Champion, A.Dandridge, G.H.Meeton: Faraday Discuss. Chem. Soc. **66**, 266 (1978)
4.178 L.Liebert, L.Strzelecki, D.VanLuyen, A.M.Levelut: Eur. Polym. J. **17**, 71 (1981)
4.179 G.Maret, A.Blumstein, S.Vilasager: Polym. Prepr. Am. Chem. Soc. Dir. Polym. Chem. **22**, 246 (1981)
4.180 C.Noel, L.Monnevie, M.F.Achard, F.Hardouin, G.Sigaud, H.Gasparoux: Polym. **22**, 578 (1981)
4.181 F.Volino, A.F.Martins, R.B.Blumstein, A.Blumstein: C. R. Acad. Sci. Paris **292**, 829 (1981)
4.182 G.Maret, F.Volino, R.B.Blumstein, A.F.Martins, A.Blumstein: Proceed. 27th Int. Symp. Macromolec. (IUPAC), Strasbourg 1981
G.Maret: Polym. Prepr. **24**(2), 249 (1983)
4.183 A.Blumstein, S.Vilasagar, S.Ponrathnam, S.B.Clough, R.B.Blumstein, G.Maret: J. Polym. Sci. Polym. Phys. Ed. **20**, 877 (1982)
4.184 F.Hardouin, M.F.Achard, H.Gasparoux, L.Liebert, L.Strzelecki: J. Polym. Sci. Polym. Phys. Ed. **20**, 975 (1982)
4.185 G.Maret, A.Blumstein: Molec. Cryst. Liq. Cryst.: **88**, 295 (1982)
4.186 S.Chandrasekhar: *Liquid Crystals* (Cambridge Univ. Press, Cambridge 1977)
4.187 V.Tsvetkov: Acta Phys. Chim. **19**, 86 (1944)

4.188 T.W.Stinson, J.D.Litster: Phys. Rev. Lett. **25**, 503 (1970)
4.189 J.C.Filippini, Y.Poggi, G.Maret: Colloq. Int. CNRS, *Physique Sous Champs Magnétiques Intenses*, **242**, 67 (1975)
4.190 J.C.Filippini, Y.Poggi: J. Physique Lett. **37**, L17, L97 (1976)
4.191 B.Malraison, Y.Poggi, J.C.Filippini: Solid. State Commun. **31**, 843 (1979)
4.192 P.H.Keyes, J.R.Shane: Phys. Rev. Lett. **42**, 722 (1979)
4.193 C.Rosenblatt: Phys. Rev. **A24**, 2236 (1981)
4.194 Y.Poggi, J.C.Filippini: Phys. Rev. Lett. **39**, 150 (1977)
4.195 B.Malraison, Y.Poggi, E.Guyon: Phys. Rev. **A21**, 1012 (1980)
4.196 B.Malraison: C. R. Acad. Sci. Paris **286B**, 307 (1978)
4.197 Y.Poggi, A.Aleonard, J.Robert: Phys. Lett. **54A**, 393 (1975)
4.198 I.Sakurai, Y.Kawamura, A.Ikegami, S.Iwayangi: Proc. Natl. Acad. Sci. 77, 7232 (1980)
4.199 E.Boroske, W.Helfrich: Biophys. J. **24**, 863 (1976)
4.200 P.G. de Gennes, C.Taupin: Private communication
4.201 W.Helfrich: Phys. Lett. **43A**, 409 (1973)
4.202 W.Helfrich: Z. Naturforsch. **28C**, 693 (1973)
4.203 C.T.Meyer, Y.Poggi, G.Maret: J. Physique **43**, 827 (1982)
4.204 B.C.Gaffney, H.M.McConnell: Chem. Phys. Let. **24**, 310 (1974)
4.205 E.Meirovitch, J.H.Freed: J. Chem. Phys. **84**, 3295 (1980)
4.206 K.D.Lawson, T.J.Flautt: J. Am. Chem. Soc. **89**, 5490 (1967)
4.207 P.C.Isolani, L.W.Reeves, J.A.Vanin: Can. J. Chem. **57**, 1108 (1979)
4.208 J.Charvolin, A.M.Levelut, E.T.Samulski: J. Physique Lett. **40**, L587 (1979)
4.209 L.Q.Amaral, C.A.Pimentel, M.R.Tavares, J.A.Vanin: J. Chem. Phys. **71**, 2940 (1979)
4.210 J.Charvolin, Y.Hendrikx: J. Physique Lett. **41**, L597 (1980)
4.211 L.B.Johansson, O.Söderman, K.Fontell, G.Lindblom: J. Phys. Chem. **85**, 3694 (1981)
4.212 L.Liebert; A.Martinet: J. Physique Lett. **40**, L363 (1979)
4.213 L.Auvray: C. R. Acad. Sci. Paris **292**, 821 (1981)
4.214 G.Porte, Y.Poggi: In *Nonlinear Behaviour of Molecules, Atoms and Ions in Electric, Magnetic and Electromagnetic Fields*, ed. by L.Neel (Elsevier, Amsterdam 1979) p. 457
4.215 G.Porte, Y.Poggi: Phys. Rev. Lett. **41**, 1481 (1978)
4.216 G.Porte, J.Appell, Y.Poggi: J. Phys. Chem. **84**, 3105 (1980)
4.217 J.Appell, G.Porte, Y.Poggi: J. Colloid. Interface Sci. **87**, 492 (1982)
4.218 C.T.Meyer, Y.Poggi, G.Maret: J. Physique **43**, 827 (1982)
4.219 E.Meirovitch, J.H.Freed: J. Phys. Chem. **84**, 3295 (1980)
4.220 G.Maret, F.Cuault-Porte, A.Mayer, P.M.Vignais: Unpublished
4.221 R.Chagneux, N.Chalazonitis: C. R. Acad. Sci. **274D**, 317 (1972)
4.222 N.Chalazonitis, R.Chagneux: C. R. Acad. Sci. **275D**, 487 (1972)
4.223 R.Chagneux, H.Chagneux, N.Chalazonitis: Biophys. J. **18**, 125 (1977)
4.224 M.Chabre: Proc. Natl. Acad. Sci. USA **75**, 5471 (1978)
4.225 M.Michel-Villaz, H.R.Saibil, N.Chabre: Proc. Natl. Acad. Sci. USA **76**, 4405 (1979)
4.226 J.F.Becker, F.Trentacosti, N.E.Geacintov: Photochem. Photobiol. **27**, 51 (1978)
4.227 F.Hong: Biophys. J. **29**, 343 (1980)
4.228 H.Saibil, M.Chabre, D.Worcester: Nature **262**, 266 (1976)
4.229 M.Michel-Villaz, C.Roche, M.Chabre: Biophys. J. **37**, 603 (1982)
4.230 F.T.Hong: J. Coll. Interface Sci. **58**, 471 (1977)
4.231 R.S.Knox, M.A.Davidovich: Biophys. J. **24**, 689 (1978)
4.232 J.F.Becker, N.E.Geacintov, F. van Nostrand, R. van Metter: Biochem. Biophys. Res. Comm. **51**, 597 (1973)
4.233 J.Breton, M.Michel-Villaz, G.Paillotin: Biochim. Biophys. Acta **314**, 42 (1973)
4.234 N.E.Geacintov, F. van Nostrand, J.F.Becker: Biochim. Biophys. Acta **347**, 443 (1974)
4.235 J.Breton, P.Mathis: Biochem. Biophys. Res. Comm. **58**, 1071 (1974)
4.236 J.Breton, E.Roux, J.Whitmarsh: Biochem. Biophys. Res. Comm. **64**, 1274 (1975)
4.237 J.Garab, J.Breton: Biochem. Biophys. Res. Comm. **71**, 1095 (1976)
4.238 A.Vermeglio, J.Breton, P.Mathis: J. Supramol. Struct. **5**, 109 (1976)
4.239 J.F.Becker, J.Breton, N.E.Geacintov, F.Trentacosti: Biochim. Biophys. Acta **440**, 531 (1976)

4.240 J.Breton, G.Paillotin: Biochim. Biophys. Acta **459**, 58 (1977)
4.241 J.Breton: Biochim. Biophys. Acta **459**, 66 (1977)
4.242 J.D.Clement-Metral: FEBS Lett. **50**, 257 (1975)
4.243 D.M.Sadler: FEBS Lett. **67**, 289 (1976)
4.244 D.C.Neugebauer, A.E.Blaurock, D.L.Worcester: FEBS Lett. **78**, 31 (1977)
4.245 M.Tricot, C.Houssier: "Electrooptical Properties of Synthetic Polyelectrolytes", in *Polyelectrolytes*, ed. by K.C.Frisch, D.Klempner, A.V.Patsid (Technomic, Westport 1976)
4.246 a R.Oberthür, G.Maret, M.Showe: To be published
b J.Torbet: EMBO J. **2**, 63 (1983)
4.247 A.Dobek, A.Patkowski, D.Labuda: J. Polym. Sci. Polym. Symp. **61**, 111 (1977)
4.248 G.Maret, R.Oldenbourg: Unpublished
4.249 J.M.Freyssinet, J.Torbet, G.Hudry Clergeon, G.Maret: Proc. Natl. Acad. Sci. USA **80**, 1616 (1983)
4.250 M.Murayama: Nature **206**, 420 (1965)
4.251 P.Costa Ribeiro, M.A.Davidovich, E.Wajnberg, G.Bemski, M.Kischinevsky: Biophys. J. **36**, 443 (1981)
4.252 A.Leitmannova, R.Stösser, R.Glaser: Stud. Biophys. **60**, 73 (1976)
4.253 G.Maret, A.Mayer: Unpublished
4.254 J.Torbet, M.Y.Norton: FEBS Lett. **147**, 201 (1982)
4.255 C.Nave, A.G.Fowler, S.Malsey, D.A.Marvin, H.Siegrist, E.J.Wachtel: Nature **281**, 232 (1979)
4.256 A.Avirom: Polymer Lett. Ed. **14**, 757 (1976)
4.257 L.Liebert, L.Strzelecki: C. R. Acad. Sci. Paris **276C**, 647 (1973)
4.258 S.B.Clough, A.Blumstein, E.C.Hsu: Macromolecules **9**, 123 (1976)
4.259 F.Cser: J. Physique Suppl. **40**, C3-459 (1979)
4.260 H.J.Lorkowski, F.Reuther: Plaste Kautsch. **23**, 81 (1976)
4.261 J.Wojtczak: Chem. Stosowana **4**, 387 (1958)
4.262 D.R.Kalkwarf, J.C.Langford: In *Biological Effects of External Low Frequency Electromagnetic Fields*, ed. by R.D.Phillips et al., DOE Symp. Ser. **50**, 408 (1979)
4.263 J.A.Oberteuffer: IEEE Trans. Magn. **9**, 303 (1973)
4.264 J.P.H.Watson: J. Appl. Phys. **44**, 4209 (1973)
4.265 S.J.Gill, C.P.Malone, M.Downing: Rev. Sci. Instrum. **31**, 1299 (1960)
4.266 S.J.Gill, C.P.Malone: Rev. Sci. Instrum. **34**, 788 (1963)
4.267 H.Kolm, J.Oberteuffer, D.Kelland: Sci. Am. **46** (Nov. 1975)
4.268 F.Paul, S.Roath, D.Melville: Br. J. Haematol. **38**, 273 (1978)
4.269 A.Porath-Furedi, P.Yanai: J. Histochem. Cyctochem. **27**, 371 (1979)
4.270 G.Bitton, R.Mitchell: Water Res. **8**, 549 (1974)
4.271 K.Mosbach, L.Andersson: Nature **270**, 259 (1978)
4.272 P.L.Kronick, G.L.Campbell, K.Joseph: Science **200**, 1074 (1978)
4.273 K.Mosbach, U.Schroeder: FEBS Lett. **102**, 112 (1979)
4.274 C.H.Evans, W.P.Tew: Science **213**, 653 (1981)
4.275 S.J.St.Lorant: "Biomagnetism, A Review", Proc. 6th Int. Conf. Magn. Techn. (MT6), (Alfa, Bratislava 1978) p. 337
4.276 D.D.Mahlum: Battelle Pacific Northwest Lab. Report, No. BNWL-1973/UC-20 (1976)
4.277 H.Martin, M.Lindauer: Fortschritte Zool. **21**, 210 (1973)
4.278 H.Aceto, C.A.Tobias, I.L.Silver: IEEE Trans. Magn. **6**, 368 (1970)
4.279 E.H.Frei: IEEE Trans. Magn. **8**, 407 (1972)
4.280 S.J.Williamson, L.Kaufmann, D.Brenner: *Superconductor Applications: Squids and Machines*, ed. by B.B.Schwartz, S.Foner (Plenum, New York 1977)
4.281 D.B.Geselowitz: IEEE Trans. Biomed. Eng. **26**, 497 (1979)
4.282 J.D.Palmer: Nature **198**, 1061 (1963)
4.283 R.Blakemore: Science **190**, 377 (1975)
R.B.Frankel, R.P.Blakemore: J. Magn. Magn. Mat. **15–18**, 1562 (1980)
R.B.Frankel, R.P.Blakemore, R.S.Wolfe: Science **203**, 1355 (1979)

4.284 R.B.Frankel, R.P.Blakemore: J. Magn. Magn. Mater. **15–18**, 1562 (1980)
4.285 J.L.Kirschvink: J. Exp. Biol. **86**, 345 (1980)
4.286 N.D.Gottlieb, W.E.Caldwell: J. Genet. Psychol. **111**, 85 (1967)
4.287 J.B.Phillips, K.Adler: In Ref. 4.130, p. 325
4.288 H.D.Picton: Nature **211**, 303 (1966)
4.289 M.C.Arendse: Nature **274**, 358 (1978)
4.290 M.Lindauer, H.Martin: In *Animal Orientation and Navigation*, ed. by S.R.Galler, K.Schmidt-Koenig, G.J.Jakobs, R.E.Belleville (Nasa SP-262, 1972) p. 559
4.291 M.Kisliuk, J.S.Ishay: Experientia **35**, 1041 (1979)
4.292 J.Zoeger, J.R.Dunn, M.Fuller: Science **213** 892 (1981)
4.293 D.P.O'Leary, J.Vilches-Troya, R.F.Dunn, A.Campoz-Munoz: Experientia **37**, 86 (1981)
4.294 A.J.Kalmijn: Oceanus **20**, 45 (1977)
A.J.Kalmijn: IEEE Trans. Mag. **MAG-17**, 1113 (1981)
4.295 R.L.Jungermann, B.Rosenblum: J,. Theor. Biol. **87**, 25 (1980)
4.296 W.Wilschko, R.Wilschko: Science **176**, 62 (1971)
4.297 W.Wilschko, R.Wilschko: Z.Tierpsychologie **37**, 337 (1975)
4.298 S.T.Emlen, W.Wilschko, N.J.Demong, R.Wilschko, S.Bergmann: Science **193**, 505 (1976)
4.299 W.Viehmann: Behaviour **68**, 24 (1978)
4.300 D.Presti, J.D.Pettigrew: Nature **285**, 99 (1980)
4.301 a B.R.Moore: Nature **285**, 69 (1980)
b J.L.Gould: Nature **296**, 205 (1982); see also Nature **300**, 293 (1982)
4.302 W.T.Keeton: Proc. Natl. Acad. Sci. **68**, 102 (1971)
4.303 C.Walcott, R.P.Green: Science **184**, 180 (1974)
4.304 J.Kiepenheuer: Naturwissenschaften **65**, 113 (1978)
J.M.Barnothy: In [Ref. 4.34, Vol. II, P. 287]
4.305 C.Walcott: IEEE Transact. Magn. **16**, 1008 (1980)
4.306 R.R.Baker: New Scientist, p. 844 (Sept. 18, 1980)
4.307 R.R.Baker: Science **210**, 555 (1980)
4.308 J.L.Gould, K.B.Able: Science **212**, 1061 (1981)
4.309 J.L.Kirschvink: J. Exp. Biol. **92**, 333 (1981)
4.310 H.G.Wallraff: Oikos **30**, 188 (1978)
4.311 R.C.Gunter, S.Bamberger, G.Valvet, M.Crossin, G.Ruhenstroth-Bauer: Biophys. Struct. Mechanism **4**, 87 (1978)
M.J.M.Leask: In [Ref. 4.40, p. 318]
4.312 E.D.Yorke: J. Theor. Biol. **77**, 101 (1979)
4.313 E.D.Yorke: J. Theor. Biol. **89**, 533 (1981)
4.314 J.L.Kirschvink, J.L.Gould: Biosystems **13**, 181 (1981)
4.315 J.L.Kirschvink: Biosystems **14**, 193 (1981)
4.316 R.Ranvaud, J.Kiepenheuer, G.Maret, K.Schmid-Koenig: Submitted to J. Comp. Phys.
4.317 L.J.Audus: Nature **185**, 132 (1960)
4.318 J.C.Schwarzbacher, L.J.Audus: J. Exp. Bot. **24**, 459 (1973)
4.319 N.M.Amer, C.A.Tobias: Radiat. Res. **31**, 644 (1967)
4.320 A.Edelman, J.Teulon, I.B.Puchnalska: Biochem. Biophys. Res. Commun. **91**, 118 (1979)
4.321 J.L.Schwartz: IEEE Trans. Biomed. Eng. **25**, 467 (1978)
4.322 J.L.Schwartz: IEEE Trans. Biomed. Eng. **26**, 238 (1979)
4.323 H.K.Goswami: Nucleus **16**, 24 (1973)
4.324 H.F.Linskens, P.S.G.M.Smeets: Experientia **34**, 754 (1978)
4.325 Levengood: In [Ref. 4.279]
4.326 P.W.Neurath: Nature **219**, 1358 (1968)
4.327 M.V.Joshi, M.Z.Khan, P.S.Damle: Differentiation **10**, 39 (1978)
4.328 B.Schaarschmidt: Naturw. Rundschau **30**, 365 (1977)
4.329 H.B.Brewer: Biophys. J. **28**, 305 (1979)
4.330 L.Y.Belousova: Biofizika **10**, 365 (1965)
4.331 E.M.Korchecskii, L.S.Marochnik: Biofizika **10**, 371 (1965)

4.332 V.A.Vardanyan: Biofizika **18**, 491 (1973)
4.333 V.Kumar: Stud. Biophys. **72**, 43 (1978)
4.334 H.Gremmel, H.Wendhausen, F.Wunsch: Wiss. Mitteilungen, Universität Kiel, Radiologische Klinik (1983)
4.335 D.Sperber, R.Oldenbourg, K.Dransfeld: Naturwiss. **71**, 100 (1984)

Additional Reference

Torbet, J., Dickens, M. J.: Orientation of skeletal muscle actin in strong magnetic fields. FEBS Lett. **173**, 403 (1984)
Torbet, J., Ronziere, M. C.: Magnetic alignment of collages during self-assembly. Biochem. J. **219**, 1057 (1984)